

Supplementary Appendix for
“Attribute associations of municipal green bond yield spreads:
A demand perspective”

Contents

Appendix A	Feature definition	3
Appendix B	Data Handling	3
Appendix C	US par yield curve features	5
Appendix D	Construction of green bond yield spreads	7
Appendix E	B-Spline curves fitted to U.S. Treasury yield par curve	10
Appendix F	Association Rule Mining Methods: Apriori and Bayesian Formulations	12
Appendix F.1	Frequentist Approach: Association Rule Learning and the Apriori Algorithm	13
Appendix F.2	Probabilistic View of ARL	15
Appendix F.3	Bayesian Model Selection and Connection to Model Formulation	18
Appendix G	Labeling and attributes categories	21
Appendix G.1	Labeling process, parameters setting and model order selection	21
Appendix G.2	Threshold setting for the Apriori Algorithm	22
Appendix G.3	Bayesian model selection (BMS)	23
Appendix H	ANOVA method and results	23
Appendix H.1	Samples	24
Appendix H.2	Hypotheses	24
Appendix H.3	Boxplot for spread variations	26

Appendix I	Parallel coordination for higher-order and extreme spreads	28
Appendix I.1	Parallel coordination for higher-order	28
Appendix I.2	Parallel coordination for extreme spreads	29
Appendix J	Assessment within bonds with specific attributes	29
Appendix J.1	Assessment within bonds with specific attributes	29
Appendix J.1.1	Callability-based attribute associations	29
Appendix J.1.2	Tax-based attribute associations	30
Appendix J.1.3	Attribute associations based on bond's issuer sector	31
Appendix J.2	UOP definition	35
Appendix J.2.1	UOP-based attribute associations	35
Appendix K	Regression model plots and tests	38
Appendix K.1	Issue date interval analysis	38
Appendix K.2	Correlation heatmaps for bonds groups.	40
Appendix K.3	Tests and diagnostic plots	41
Appendix K.4	Results and diagnostic plots for N3_2 and N3_3	42

Appendix A. Feature definition

This appendix outlines the definitions of the green bond attributes obtained from the Bloomberg terminal.

Table A.1: Description of attributes

Type	Attributes	Description
Categorical	ID_CUSIP	Security identification number for the U.S. and Canada. The Committee on Uniform Security Identification Procedures (CUSIP) number consists of nine alphanumeric characters. The first six characters identify the issuer, the following two identify the issue, and the final character is a check digit.
	MUNI_TAX_PROV	Describes the United States (U.S.) federal and state income tax status of the bond. Will designate if a bond is subject to Federal Tax or Alternative Minimum Tax (AMT), or if the bond is Bank Qualified. Additionally, field may return whether the bond is subject to state income tax.
	CPN_TYP	Specifies how the periodic payment is structured. Under specific scenarios, payment structure details are replaced with information detailing the state of the instrument (Defaulted, Exchanged, Flat Trading, Funged, Prelim, When Issued).
	CRNCY	Currency in which the security was issued.
	ISSUER_BULK	The full name of the issuing entity of the security.
	SELF_REPTD_GREEN_INSTR_INDCTR	Indicates that the issuer has self-reported that the net proceeds of the fixed income instrument will be applied toward green projects or activities that promote climate change mitigation or adaptation, or other environmental sustainability purposes.
	BB_COMPOSITE	Blend of a security's Moody's, S&P, Fitch, and DBRS ratings.
	MUNI_LONG_INDUSTRY_TYP	Full name of industry sector bonds.
	CALLABLE	Indicates whether the security has a call provision.
	MARKET_ISSUE	Market in which the bond was issued.
Numerical	MUNI_PURPOSE	Describes how the proceeds of the bonds are being used.
	FINANCING_TYPE	Identifies whether the municipal bond's proceeds were used as money for new projects ('New Money'), refunding/refinancing of prior debt, or a combination of such types.
	State Code	State code associated with the issuer of the security.
	CPN_FREQ	Number of times per year interest is paid.
	CPN	Current interest rate of the security.
	ISSUE_DT	Date the security is issued.
	MATURITY	Date the principal of a security is due and payable.
	SPREAD_AT_ISSUANCE_TO_WORST	Spread for tax-exempt bonds is calculated from Bloomberg Valuation Service (BVAL) AAA (I493) curve for deals brought to market before 9/25/17; and from Bloomberg Valuation Service (BVAL) AAA Callable (BS1211) curve thereafter. Spread is calculated to appropriate interpolated point on the curve. Modified Duration for Non-Mortgages based on the Mid Price (PR003, PX_MID) of the security is returned.
	DUR_ADJ_MID	
	YIELD_ON_ISSUE_DATE	The yield the bond offered on the issue date. This field is not available for variable rate demand obligations (VRDOs).
	ISSUE_PX	Price of the security at issue.
	AMT_ISSUED	Cumulative amount issued from the original security pricing date through to the current date for debt securities.
	MUNI_ISSUE_SIZE	Returns the aggregate of the entire deal size (in USD), comprising all the series of bonds brought to market by the same lead underwriter in the deal to which the security belongs as detailed in the official statement.
	MTY_YEARS	The number of years until the principal amount becomes due.

Appendix B. Data Handling

Outlier handling

To address potential outliers in the ‘yield’ variable, a two-step iterative process based on Z-scores is employed. Initially, Z-scores are calculated for each yield observation. Data

points with absolute Z-scores exceeding a threshold of 3 are identified as potential outliers and systematically removed from the dataset. Following this initial removal, Z-scores are recalculated for the remaining ‘yield’ values. This approach allowed for a step-wise identification and removal of potential outliers, providing a systematic means to address extreme values in the ‘yield’ variable. The iterative nature of the process enabled a controlled adjustment of the dataset while considering the impact on statistical properties. Moreover, implementing this method will result in the removal of approximately 0.05% of the data, suggesting that it is a suitable approach for preserving data integrity.

The table below presents a statistical summary of yield observations in California following the application of each step.

Table B.1: Summary statistics for yield at each step of outlier handling

Steps	Descriptive Statistics					
	Min.	1st Qu.	Median	Mean	3rd Qu.	Max.
Initial Dataset	-117.062	2.104	2.893	3.123	3.684	23858.704
First Step	-106.321	2.104	2.892	2.950	3.683	116.527
Second Step	-1.900	2.099	2.885	2.892	3.671	8.613

The following plots show the distribution of observed yield in each step.

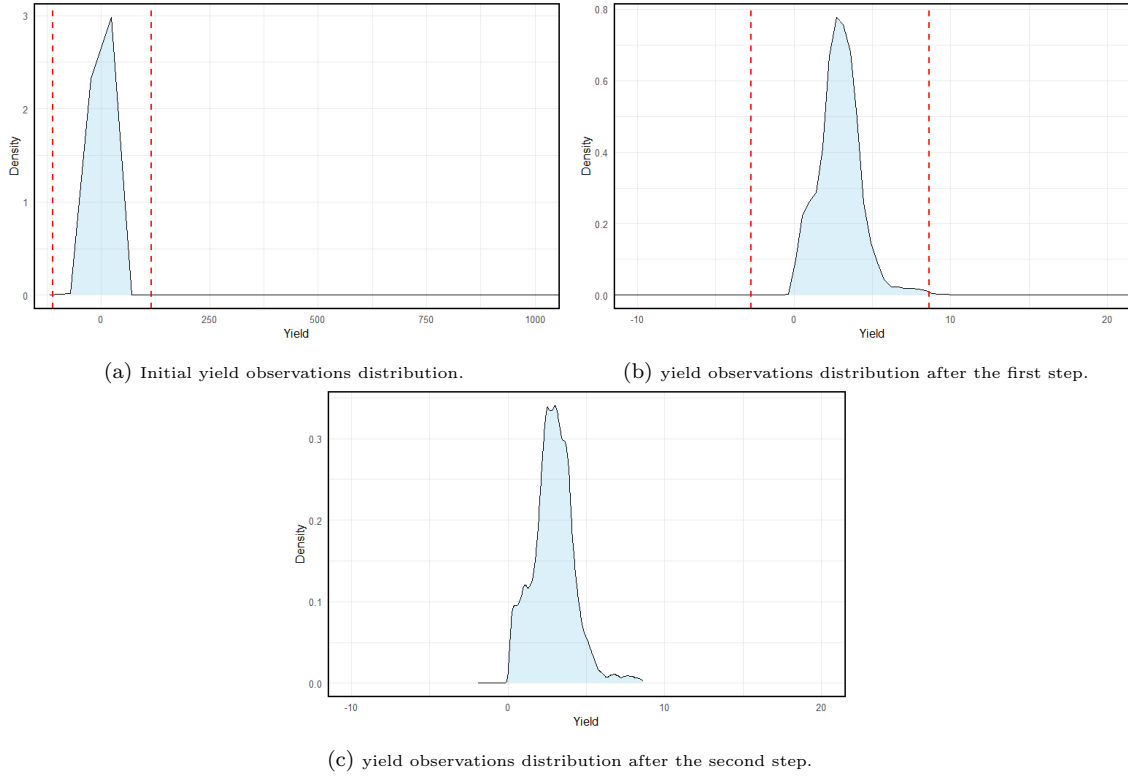


Figure B.1: Distribution of yields

This figure shows the distribution of observed yield in California through outliers handling steps. Red horizontal dashed lines represent ± 3 Z-score thresholds.

Appendix C. US par yield curve features

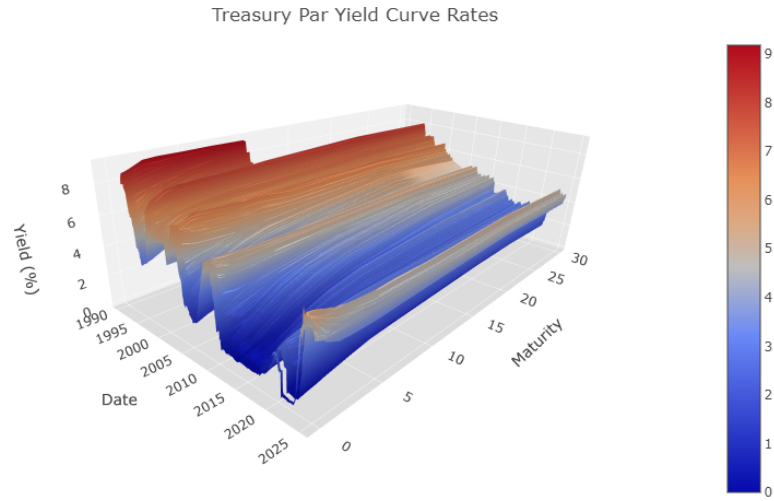


Figure C.1: U.S treasury par yields

This figure depicts the dynamic evolution of U.S treasury par yields between 1990-2024.

Fig. C.1 presents the dynamic evolution of U.S Par yields over time.

To enhance our understanding of the behavior of green bond spreads, we investigate features of the U.S. par yield curve, including convexity and gradient.

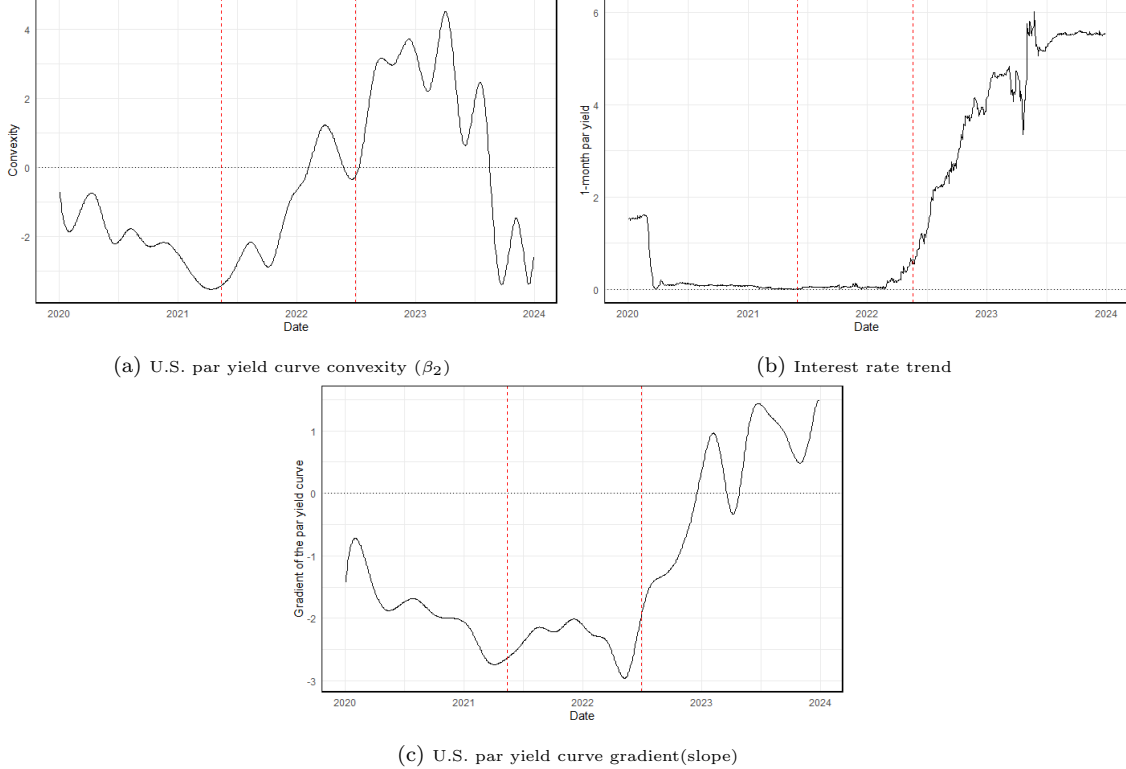


Figure C.2: **US par yield convexity and interest rate.**

This figure shows the convexity and slope of U.S. par yield curve and 1-month yield trend within 2020-2023. Two vertical dashed lines mark the dates 2021-05-13 and 2022-09-06.

Thus, we apply the Nelson-Siegel model to the daily rates of different tenors of the U.S. par yield curve, which serve as the reference rates in the spreads calculations, specifically,

$$Y(\tau) = \beta_0 + \beta_1 (1 - e^{-\frac{\tau}{\lambda}}) + \beta_2 \left(\frac{\tau}{\lambda} - e^{-\frac{\tau}{\lambda}} \right),$$

where β_0 , β_1 , and β_2 represent the level, slope, and curvature of the yield curve, respectively. Note that, β_0 captures long-term average interest rates, β_1 reflects the speed of short-term rates converging to the long-term average, and β_2 denotes the convexity of the yield curve, indicating deviations from linearity in the relationship between maturity and yield (Diebold and Li, 2006).

We use 30 cubic B-splines to smooth these coefficients. We then plot smoothed β_2 and β_1 , representing the yield curve's convexity and gradient. We include the 1-month U.S. Treasury

par yields to reflect market expectations of interest rates. Figure C.2 displays the convexity and slope (gradient) of the U.S. par yield curve alongside the prevailing interest rate regime within the specified interval.

Calculation of remaining time to maturity

As outlined in subsection 2.1.1 of the main paper, our methodology adopts a dynamic approach with a daily frequency. To capture the evolving trend of bonds' yields, it is necessary to update both τ_n and τ_N . These terms undergo continuous updates throughout the dataset's entire time span, following the Actual/Actual day count convention. Actual/Actual or ACT/ACT calculates the daily interest using the actual number of days in the year and then multiplies that by the actual number of days in each time period. The U.S. Treasury bonds and municipal green and conventional bonds use this convention in calculations of rates day count convention.

Appendix D. Construction of green bond yield spreads

Firstly, we use the observed daily YTM of green bonds and a risk-free reference yield, such as the U.S. Treasury par yield, to discount the respective cash flows of the bonds to compute synthetic green and conventional bond prices. We then use these synthetic bond prices to compute the green and reference equivalent Zero-Coupon Bond Yields to Maturity (ZCBYTM).

More specifically, we compute the value of a green bond i by using the YTM of this green bond to discount its cash flows. Thus, all the cash flows of a green bond are discounted by the same fixed rate – its YTM. The value of this bond is then used to compute the equivalent green ZCBYTM. The corresponding reference rate from a risk-free yield curve is selected, so it matches the tenor of the green bond i . We use this reference rate as the fixed rate to discount the (same) cash flows to determine the equivalent risk-free ZCBYTM. The difference between green ZCBYTM and risk-free ZCBYTM determines the spread of green bond i .

- **Green Equivalent ZCBYTM_s**

We consider green bond i at time t with coupon amount C_i , face value (par amount)

FV_i , coupon frequency m_i , and annualized $YTM_{i,t}^G$, which has payments in \hat{N} periods from first issuance over the entire term of the bond and in N periods according to the remaining time to maturity. As we propose a dynamic approach on a daily basis, we define $\tau_{i,n}$ representing the remaining year fraction to the n^{th} payment at time t for bond i as follows:

$$\tau_{i,n} := \max \left\{ n - \frac{t}{(365/m_i)}, 0 \right\}. \quad (\text{D.1})$$

We also define the indicator function as follows:

$$\mathbb{I}(\tau_{i,n}) := \begin{cases} 1, & \text{if } \tau_{i,n} > 0, \\ 0, & \text{otherwise.} \end{cases} \quad (\text{D.2})$$

When $\tau_{i,n}$ reaches zero, it signifies that we have either reached or exceeded the coupon payment date for coupon i . At this point, the indicator function will be employed to exclude previously paid coupons from the calculation.

Thus, we calculate equivalent green ZCBYTM s at time t for bond i , denoted as $YTM_{i,t}^{(GZCB)}$ according to the following steps:

1. Calculate the present value of bond i at time t denoted as $P_{i,t}$ as follows:

$$P_{i,t} = \sum_{n=1}^N \frac{C_i \mathbb{I}(\tau_{i,n})}{(1 + YTM_{i,t}^{(G)})^{\tau_{i,n}}} + \frac{FV_i}{(1 + YTM_{i,t}^{(G)})^{\tau_{i,N}}}. \quad (\text{D.3})$$

2. Define an equivalent zero-coupon bond, characterized by a face value denoted as \widetilde{FV}_i . The face value of the equivalent zero coupon bond i is defined as follows:

$$\widetilde{FV}_i := \max \left\{ FV_i, FV_i + C_i \right\}. \quad (\text{D.4})$$

\widetilde{FV}_i is adjusted for bonds that pay both a coupon and par amount on the maturity date. This adjustment is important for bonds where the final coupon is paid at maturity, as it ensures that the equivalent zero-coupon bond properly accounts for the entire cash flow structure. It is defined as the maximum of the original bond's FV or $FV + C$ if there's a coupon on the last day. Subsequently the present value of the equivalent zero coupon bond i at time t , $P_{i,t}^{ZCB}$ is defined as:

$$P_{i,t}^{ZCB} = \frac{\widetilde{FV}_i}{(1 + YTM_{i,t}^{(GZCB)})^{\tau_{i,N}}}. \quad (\text{D.5})$$

3. Equate $P_{i,t}$ to $P_{i,t}^{ZCB}$ and rearranging, we can obtain $YTM_{i,t}^{(GZCB)}$ as follows :

$$\frac{\widetilde{FV}_i}{(1 + YTM_{i,t}^{(GZCB)})^{\tau_{i,N}}} = \sum_{n=1}^N \frac{C_i \mathbb{I}(\tau_{i,n})}{(1 + YTM_{i,t}^{(G)})^{\tau_{i,n}}} + \frac{FV_i}{(1 + YTM_{i,t}^{(G)})^{\tau_{i,N}}}, \quad (\text{D.6})$$

$$YTM_{i,t}^{(GZCB)} = \left[\frac{1}{\widetilde{FV}_i} \left(\sum_{n=1}^N \frac{C_i \mathbb{I}(\tau_{i,n})}{(1 + YTM_{i,t}^{(G)})^{\tau_{i,n}}} + \frac{FV_i}{(1 + YTM_{i,t}^{(G)})^{\tau_{i,N}}} \right) \right]^{-\frac{1}{\tau_{i,N}}} - 1. \quad (\text{D.7})$$

- **Reference equivalent ZCBYTM**

We compute a reference equivalent ZCBYTM rate, denoted as $YTM_{i,t}^{(RZCB)}$, using a reference risk-free rate. Discounting rates are derived from the fitted spline curves of annual reference rates at time t , based on the same tenor used in the green ZCBYTM calculation. These rates are applied similarly to the previous stage, discounting the associated cash flows as follows:

$$YTM_{i,t}^{(RZCB)} = \left[\frac{1}{\widetilde{FV}_i} \left(\sum_{n=1}^N \frac{C_i \mathbb{I}(\tau_{i,n})}{(1 + r_t^{(Tr)}(\tau_{i,N}))^{\tau_{i,n}}} + \frac{FV_i}{(1 + r_t^{(Tr)}(\tau_{i,N}))^{\tau_{i,N}}} \right) \right]^{-\frac{1}{\tau_{i,N}}} - 1, \quad (\text{D.8})$$

where $r_t^{(Tr)}(\tau_{i,N})$ is the corresponding reference rate for $\tau_{i,N}$ year(s) maturity bond at time t and $YTM_{i,t}^{(RZCB)}$ is the reference equivalent ZCBYTM rate of the bond i at time t corresponding to the discount factor $r_t^{(Tr)}(\tau_{i,N})$.

- **Spread Calculation**

Once the $YTM_{i,t}^{(GZCB)}$ and $YTM_{i,t}^{(RZCB)}$ have been determined, we can determine the daily spread based on YTM. We define the non-parametric $S_{i,t}$ as follows: ¹

¹We opt to define a YTMZCB corresponding to the reference rate $r_t^{(Tr)}(\tau_{i,N})$, as opposed to a direct comparison of this rate ($r_t^{(Tr)}(\tau_{i,N})$) with the $YTM_{i,t}^{(RZCB)}$. This approach allows us to capture specific bond characteristics, including coupon rate, coupon frequency, and maturity, through defining a reference rate. From a mathematical standpoint, the rationale lies in dealing with a non-linear (hyperbolic) transformation of rates. It is important to note that the input rate ($r_t^{(Tr)}(\tau_{i,N})$) undergoes a non-linear transformation, and this discrepancy with $YTM_{i,t}^{(RZCB)}$ becomes more pronounced, especially as the maturity period extends.

$$S_{i,t} := YTM_{i,t}^{(GZCB)} - YTM_{i,t}^{(RZCB)}. \quad (\text{D.9})$$

Essentially, the tenor-specific approach uses a single matching tenor point on the green and reference yield curves and compares a time series of green ZCBYTM with a time series of risk-free ZCBYTM at the same tenor point to obtain the spread of the green bond i . We repeat this method for all green bonds on day t , and consequently compute the spread for all available green bonds on this day.

Figure D.1 presents the median of the daily green bond yield spread (computed as described above) for 2013–2024. Since relatively few bonds were issued before 2016, the median becomes highly noisy and may reduce the accuracy of the results. To address this, we begin our sample interval in 2016.

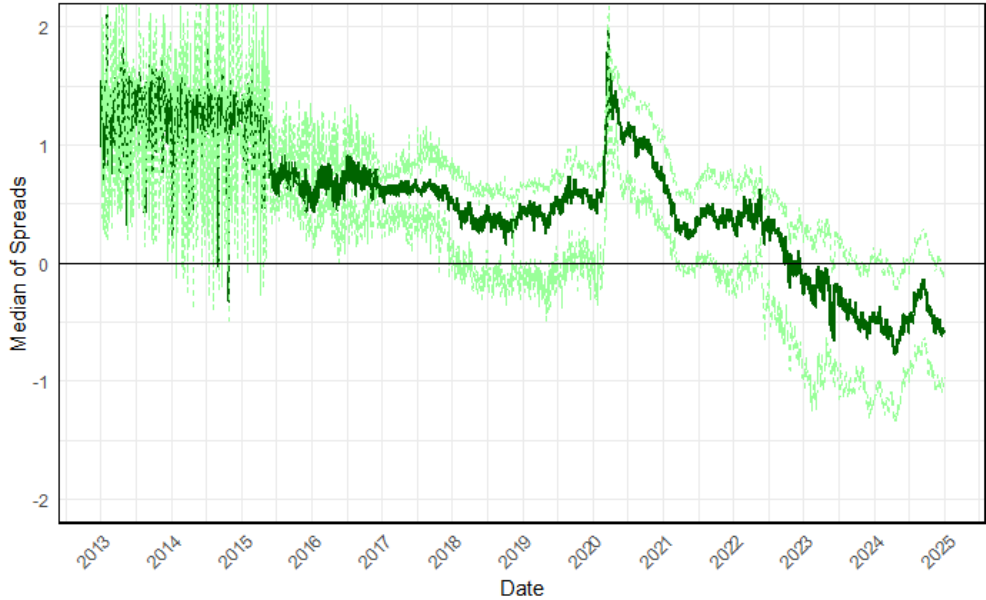


Figure D.1: Green bond yield spreads based on yield-to-maturity (YTM). The figure shows the daily median of California green bond yield spreads, denoted as S , over the period 2013–2024. The series appears relatively noisy prior to 2016 due to the limited number of bond issuances. The green dashed lines indicate the 25th and 75th percentiles of S .

Appendix E. B-Spline curves fitted to U.S. Treasury yield par curve

B-Spline curves are a mathematical representation commonly used for estimating yield curves. The term “spline” refers to a flexible strip used to manually draw smooth curves, and “Basis” indicates that the curve is constructed as a linear combination of basis functions.

B-Spline curves are particularly useful for capturing complex movements and irregularities in yield curves over different maturities ([Yallup, 2012](#)). More specifically, B-spline curves provide flexibility in representing the shape of the yield curve, allowing for a smooth and continuous representation. The degree of smoothness is controlled by the order of the B-Spline curve, with higher orders producing more flexibility but also requiring more control points. Control points or knots act as anchor points that influence the shape of the curve, and the basis functions dictate how each control point contributes to the overall curve. Cubic splines are optimal in minimizing Mean Squared Error (MSE), see ([Hastie et al., 2009](#)).

For demonstration purposes, Fig. [E.1](#) depicts the fitted spline curves (for order 1, 2 and 3) to the U.S. Treasury yield par curve on four typical dates within each year of our study. Each row presents different degrees of splines. The fit is satisfactory and the splines capture the distinct patterns that prevail during the sample period. Order 3 splines are used for the analysis, as they offer the best fit.

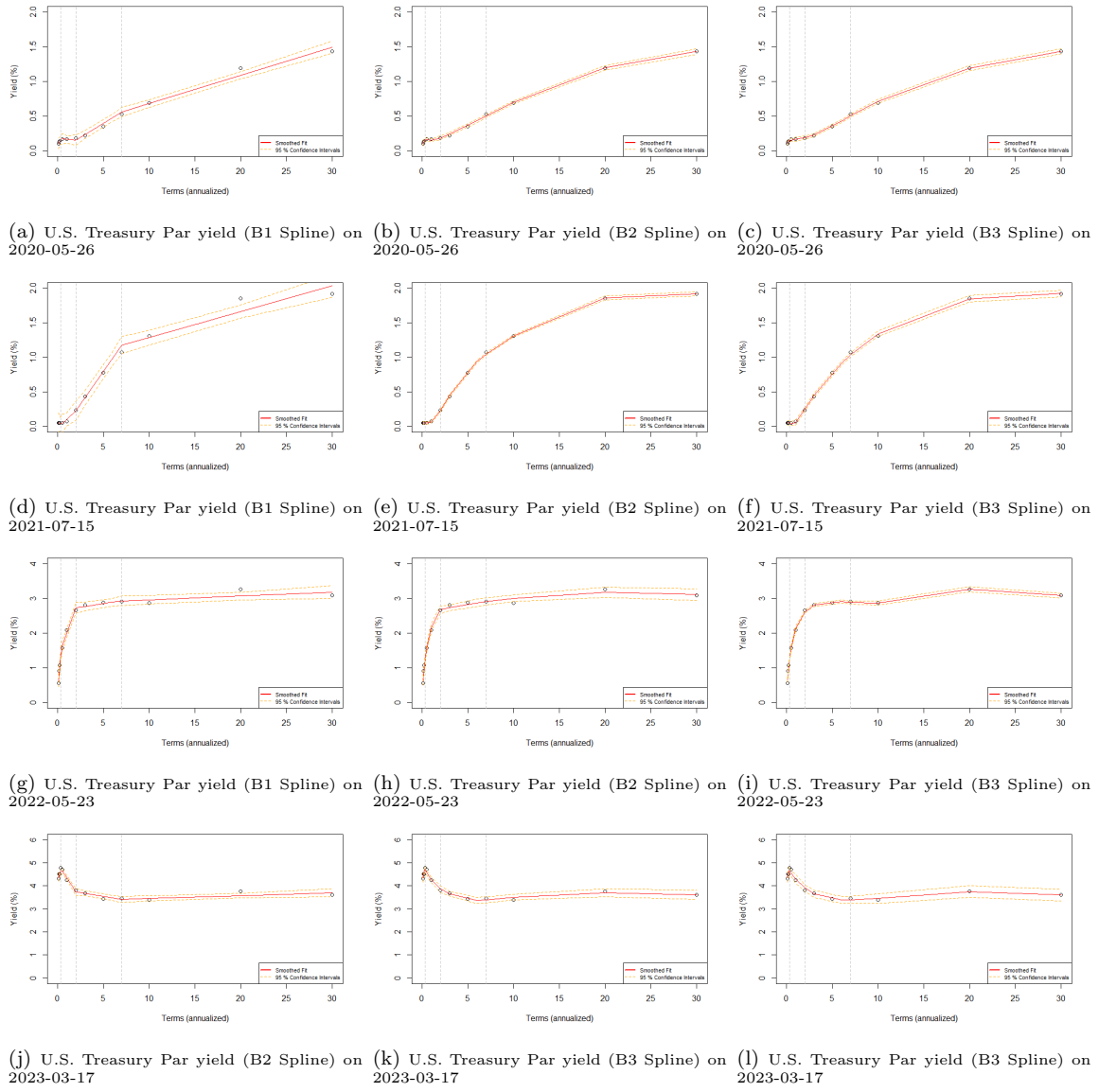


Figure E.1: **Fitted curves to the U.S. Treasury Par yield**

The figure displays B-spline curves of varying degrees fitted to the U.S. Treasury Par yield on different days across the four-year dataset interval. The red line represents the fitted B1-Spline bootstrapped curve, while the dotted orange curve depicts the 95% confidence intervals for the predicted rates. The grey vertical lines represent the control points or knots.

Appendix F. Association Rule Mining Methods: Apriori and Bayesian Formulations

Our experimental framework applies **Association Rule Learning (ARL)** [Agrawal et al. \(1993\)](#)—a machine learning technique that, when viewed through a Bayesian network structure, provides a probabilistic interpretation—to analyze green bond spreads. This approach addresses key questions central to investor screening, such as identifying bonds

with spreads that are either positive or negative relative to risk-free benchmarks (e.g., U.S. Treasuries).

Effective screening requires an analysis of both single-tenor spreads and term structures, capturing factors like bond maturity and yield curve shapes. Yield curve shapes—such as inverted, flat, or steep—reflect broader economic conditions that influence spreads based on a bond’s tenor and attributes.

Additionally, screening practices may target specific bond characteristics, such as the **Use of Proceeds (UOP)** category, which affects green bonds’ potential to meet environmental goals. For example, the UOP category (e.g., green energy vs. transportation) affects the impact of green labels, index listings, and environmental outcomes. It can also shape default and repayment risks as characteristics like tenor, maturity, callability, coupon rate, and issuer sector interact with UOP to directly influence spreads.

In the following subsections, we outline our approach, starting with a description of ARL and the Apriori algorithm. We then transition to a **Bayesian Network Interpretation** for a probabilistic understanding of ARL, leading into **Bayesian Model Selection** for interpreting results rigorously.

Appendix F.1. Frequentist Approach: Association Rule Learning and the Apriori Algorithm

Association Rule Learning (ARL) uncovers relationships between variables in a dataset, operating based on observed co-occurrence frequencies. The Apriori algorithm identifies association rules that meet predefined support and confidence thresholds [Agrawal et al. \(1993\)](#). In our green bond context, let $\{\mathbf{x}_{i,t}\}_{i=1,t=1}^{M,T}$ be our set of observations for M bonds over T time stamps, giving $N = M \times T$ total bond-time observations. Each observation represents a bond-time transaction:

$$\mathbf{x}_{i,t} = [x_{a_1}, \dots, x_{a_D}, s_{i,t}] \quad (\text{F.1})$$

where:

- $\{x_{a_1}, \dots, x_{a_D}\}$ represents the one-hot encoded categorical attributes, where D is the total number of categories across all attributes. For example:

- Rating levels: [AAA, AA, A] \rightarrow [1,0,0]

- Tax status: [Exempt, Taxable] \rightarrow [1,0]
- Coupon range: [0-3%, 3-5%, 5-8.5%] \rightarrow [0,1,0]
- $s_{i,t} \in \{0, 1\}$ indicates whether bond i at time t belongs to the specific spread category being analyzed (S+, S-, or S0)

Let $\mathcal{T} = [\mathbf{X}_A, \mathbf{s}] \in \{0, 1\}^{N \times (D+1)}$ be our transaction database where:

- Matrix $\mathbf{X}_A \in \{0, 1\}^{N \times D}$ represents all N bond-time observations across their one-hot encoded categorical attributes, where each row contains the concatenated one-hot vectors of all attributes. For a bond at time t with:

- Rating = AAA: [1,0,0]
- Tax status = Exempt: [1,0]
- Coupon = 3-5%: [0,1,0]

The corresponding row in \mathbf{X}_A would be: [1,0,0,1,0,0,1,0]

- Vector $\mathbf{s} \in \{0, 1\}^N$ indicates for each observation whether it belongs ($s_{i,t} = 1$) or not ($s_{i,t} = 0$) to the specific spread category being analyzed

An **association rule** is defined as a mapping from a set of attribute category indicators to the specific spread category. The effectiveness of these rules is evaluated using three primary metrics: **Support**, **Confidence**, and **Lift**, defined as follows:

1. The *Support* measures the proportion of bond-time observations where the attribute category combination occurs together with the analyzed spread category:

$$\text{Supp}(\mathbf{X}_A \rightarrow \mathbf{s}) = \frac{\text{count}(\mathbf{X}_A \cap \mathbf{s})}{N}, \quad (\text{F.2})$$

where $\text{count}(\mathbf{X}_A \cap \mathbf{s})$ counts observations containing both the specified attribute category indicators and the analyzed spread category ($s_{i,t} = 1$).

2. The *Confidence* indicates the reliability of the rule by measuring the proportion of transactions containing the attribute category indicators that also belong to the analyzed spread category:

$$\text{Conf}(\mathbf{X}_A \rightarrow \mathbf{s}) = \frac{\text{Supp}(\mathbf{X}_A \cap \mathbf{s})}{\text{Supp}(\mathbf{X}_A)} = \frac{\text{count}(\mathbf{X}_A \cap \mathbf{s})}{\text{count}(\mathbf{X}_A)}. \quad (\text{F.3})$$

3. The *Lift* assesses the degree of dependency between attribute category indicators and the analyzed spread category:

$$\text{Lift}(\mathbf{X}_A \rightarrow s) = \frac{\text{Conf}(\mathbf{X}_A \rightarrow s)}{\text{Supp}(s)} = \frac{\text{Supp}(\mathbf{X}_A \cap s)}{\text{Supp}(\mathbf{X}_A) \cdot \text{Supp}(s)}. \quad (\text{F.4})$$

A $\text{Lift} > 1$ indicates a positive association, $\text{Lift} = 1$ signifies independence, and $\text{Lift} < 1$ suggests a negative association between the attribute category combination and the analyzed spread category.

Appendix F.2. Probabilistic View of ARL

Bayesian methods are advantageous for handling uncertainty, small datasets, or sparse data, as they avoid overfitting by incorporating prior distributions. They also allow for a more nuanced interpretation of rules, as posterior probabilities provide a measure of the certainty of discovered associations.

The Bayesian framework in ARL provides a probabilistic interpretation of relationships between categorical bond attributes (represented in our transaction database $\mathcal{T} = [\mathbf{X}_A, s]$) and spread outcomes. While this framework can accommodate multiple outcomes, we will show how it specializes effectively to our specific case where we analyse one spread category at a time over our $N = M \times T$ bond-time observations.

By framing association rules within a Bayesian bipartite network structure, we can represent dependencies between encoded categorical indicators and spread outcomes as directed probabilistic relationships. In the general case, these relationships connect the one-hot encoded indicators of m categorical attributes to spread outcomes at different time points, while in our specific application, we analyze one spread category (S_+ , S_- , or S_0) at a time.

In this Bayesian bipartite network, one-hot encoded categorical indicators form one set of nodes, while spread outcomes form the other set. Directed edges from encoded indicators to spread outcomes represent probabilistic dependencies. This setup allows for a clear and structured representation of conditional relationships, as illustrated in Fig. F.1, where the rule connecting encoded attributes to outcomes is represented as directed edges from indicator nodes to spread nodes.

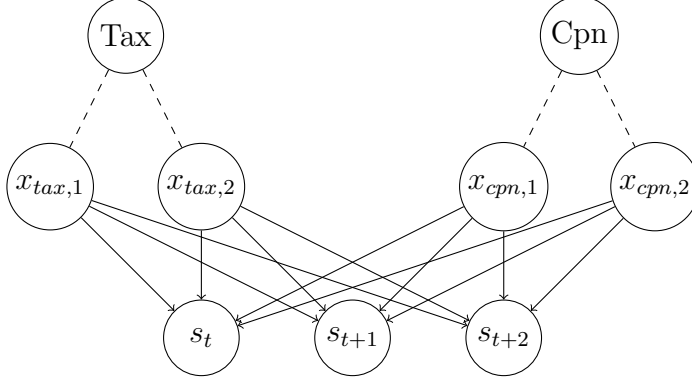


Figure F.1: **Bayesian Network Structure.** Dashed lines represent one-hot encoding relationships, while arrows represent probabilistic dependencies. Spread outcomes s_t evolves across time.

In the general framework, for each categorical attribute a (e.g., rating, tax status), category-level priors $P(x_{a,k})$ represent the initial probabilities of observing each category k independently. For instance, for coupon categories $k \in \{1, 2, 3\}$ corresponding to ranges $\{0\text{-}3\%, 3\text{-}5\%, 5\text{-}8.5\%\}$, we assign priors $P(x_{cpn,k})$ that reflect our initial beliefs about their occurrence and importance for spread behaviour.

Each node in our network corresponds to one category of a categorical attribute, where directed links indicate parent-child relationships. The Bayesian network represents a unique joint probability distribution:

$$P(x_{1,k_1}, \dots, x_{m,k_m}, s) = \prod_{i=1}^n P(x_{i,k_i} | Pa(x_{i,k_i})) \quad (\text{F.5})$$

where x_{i,k_i} represents category k_i of attribute i , and s is the spread outcome.

With category priors, the general Bayesian probabilistic view can be represented as:

$$\begin{aligned} P(x_{1,k_1}, \dots, x_{m,k_m}, s) &= \prod_{i=1}^m P(x_{i,k_i}) P(s | x_{1,k_1}, \dots, x_{m,k_m}) \\ &= \prod_{i=1}^m \text{Supp}(x_{i,k_i}) \frac{P(\{s, x_{1,k_1}, \dots, x_{m,k_m}\})}{P(x_{1,k_1}, \dots, x_{m,k_m})} \end{aligned} \quad (\text{F.6})$$

In our specific application to green bond spreads, since we analyze one spread category

at a time, this reduces to:

$$\begin{aligned}
P(x_{1,k_1}, \dots, x_{m,k_m}, s) &= \prod_{i=1}^m P(x_{i,k_i}) P(s \mid x_{1,k_1}, \dots, x_{m,k_m}) \\
&= \prod_{i=1}^m \text{Supp}(x_{i,k_i}) \frac{P(\{s, x_{1,k_1}, \dots, x_{m,k_m}\})}{P(x_{1,k_1}, \dots, x_{m,k_m})} \\
&= \prod_{i=1}^m \text{Supp}(x_{i,k_i}) \frac{\text{Supp}(\{s, x_{1,k_1}, \dots, x_{m,k_m}\})}{\text{Supp}(x_{1,k_1}, \dots, x_{m,k_m})}.
\end{aligned} \tag{F.7}$$

From this specialized framework, we can derive the Bayesian Confidence (BC) of a rule. For a rule involving specific categories of attributes leading to a spread outcome:

$$\begin{aligned}
\text{BC}(\{x_{1,k_1}, \dots, x_{m,k_m}\} \rightarrow s) &= P(s \mid x_{1,k_1}, \dots, x_{m,k_m}) \\
&= \frac{P(x_{1,k_1}, \dots, x_{m,k_m}, s)}{P(x_{1,k_1}, \dots, x_{m,k_m})}
\end{aligned} \tag{F.8}$$

We can incorporate a penalty for the rule's length (total number of categories involved, denoted as L):

$$\text{BC}_L(\{x_{1,k_1}, \dots, x_{m,k_m}\} \rightarrow s) = \left(\frac{P(x_{1,k_1}, \dots, x_{m,k_m}, s)}{P(x_{1,k_1}, \dots, x_{m,k_m})} \right)^{|L|} \tag{F.9}$$

To illustrate this framework, consider an association rule mapping from \mathbf{X}_A to \mathbf{s} , where \mathbf{X}_A contains specific one-hot encoded categories:

$$\begin{aligned}
\mathbf{X}_A : \{x_{tax,1} = 1 \text{ (tax-exempt)}, x_{price,2} = 1 \text{ (at-par)}, \\
x_{call,1} = 1 \text{ (callable)}, x_{cpn,2} = 1 \text{ (3-5\%)}\} \rightarrow \mathbf{s} = 1
\end{aligned}$$

The BC for this specific rule with length penalty is:

$$\text{BC}_L(\mathbf{X}_A \rightarrow \mathbf{s}) = \left(\frac{P(\mathbf{X}_A, \mathbf{s})}{\text{Supp}(\mathbf{X}_A)} \right)^{|L|} \tag{F.10}$$

where \mathbf{X}_A represents our specific combination of one-hot encoded categories.

The Bayesian Lift (BL) extends this framework by comparing conditional and marginal probabilities:

$$\begin{aligned}
\text{BL}(\mathbf{X}_A \rightarrow \mathbf{s}) &= \frac{\text{BC}(\mathbf{X}_A \rightarrow \mathbf{s})}{P(\mathbf{X}_A)P(\mathbf{s})} = \frac{P(\mathbf{X}_A, \mathbf{s})}{P(\mathbf{X}_A)P(\mathbf{s})} \\
&= \frac{P(\{x_{tax,1}, x_{price,2}, x_{call,1}, x_{cpn,2}, \mathbf{s}\})}{\prod P(x_{i,k_i})P(\mathbf{s})} \in (0, \infty)
\end{aligned} \tag{F.11}$$

The interpretation of BL provides crucial insights into the strength and nature of associations between one-hot encoded categories in \mathbf{X}_A and spread outcomes \mathbf{s} :

- When $BL = 1$, we have $\frac{P(\mathbf{s}|\mathbf{X}_A)}{P(\mathbf{s})} = 1$, equivalent to $\frac{P(\mathbf{X}_A, \mathbf{s})}{P(\mathbf{X}_A)P(\mathbf{s})} = 1$. This implies $P(\mathbf{X}_A, \mathbf{s}) = P(\mathbf{X}_A)P(\mathbf{s})$, indicating independence between the one-hot encoded categories and the spread outcome.
- When $BL > 1$, we have $\frac{P(\mathbf{s}|\mathbf{X}_A)}{P(\mathbf{s})} > 1$, which implies $P(\mathbf{X}_A, \mathbf{s}) > P(\mathbf{X}_A)P(\mathbf{s})$. This suggests that \mathbf{s} positively depends on \mathbf{X}_A , i.e., the specific combination of one-hot encoded categories is positively associated with the spread outcome.
- When $BL < 1$, we have $\frac{P(\mathbf{s}|\mathbf{X}_A)}{P(\mathbf{s})} < 1$, which means $P(\mathbf{X}_A, \mathbf{s}) < P(\mathbf{X}_A)P(\mathbf{s})$. This implies that \mathbf{s} negatively depends on \mathbf{X}_A , i.e., the specific combination of one-hot encoded categories is negatively associated with the spread outcome (Tian et al., 2013).

This specialized framework, focusing on single spread outcomes, provides a powerful tool for analyzing the relationships between combinations of bond characteristics (represented through one-hot encoded categories in \mathbf{X}_A) and spread behavior in green bond markets. The BL metric, in particular, offers clear interpretation of the strength and direction of these relationships, facilitating both theoretical understanding and practical application in bond market analysis.

Appendix F.3. Bayesian Model Selection and Connection to Model Formulation

To identify the most relevant association rules, we use **Bayesian Model Selection**, which ranks candidate models by evaluating their posterior probabilities. Consider a set of candidate rule models $\{\mathcal{M}_k^{\mathbf{X}_A \rightarrow \mathbf{s}}\}_{k \in \mathcal{K}}$, where each model $\mathcal{M}_k^{\mathbf{X}_A \rightarrow \mathbf{s}}$ contains a specific subset of association rules linking one-hot encoded bond attribute categories to spread outcomes. Here, $k \in \mathcal{K}$ indexes the space of all possible models, with each k representing a unique configuration of rules.

The posterior probability of a model given observed data D can be written as:

$$P(\mathcal{M}_k^{\mathbf{X}_A \rightarrow \mathbf{s}} | D) = \frac{p(D | \mathcal{M}_k^{\mathbf{X}_A \rightarrow \mathbf{s}})P(\mathcal{M}_k^{\mathbf{X}_A \rightarrow \mathbf{s}})}{\sum_{\ell \in \mathcal{K}} p(D | \mathcal{M}_\ell^{\mathbf{X}_A \rightarrow \mathbf{s}})P(\mathcal{M}_\ell^{\mathbf{X}_A \rightarrow \mathbf{s}})}, \quad (\text{F.12})$$

where the marginal likelihood $p(D | \mathcal{M}_k^{\mathbf{X}_A \rightarrow \mathbf{s}})$ can be computed as a sum (since we have discrete rules) over all possible rule configurations θ_k in model k :

$$p(D | \mathcal{M}_k^{\mathbf{X}_A \rightarrow \mathbf{s}}) = \sum_{\theta_k} p(D | \theta_k, \mathcal{M}_k^{\mathbf{X}_A \rightarrow \mathbf{s}})p(\theta_k | \mathcal{M}_k^{\mathbf{X}_A \rightarrow \mathbf{s}}) \quad (\text{F.13})$$

Here, θ_k represents a specific configuration of rules within model k , and the likelihood $p(D | \theta_k, \mathcal{M}_k^{\mathbf{X_A} \rightarrow \mathbf{s}})$ can be computed using the Bayesian Support and Confidence measures defined earlier:

$$p(D | \theta_k, \mathcal{M}_k^{\mathbf{X_A} \rightarrow \mathbf{s}}) = \prod_{r \in \theta_k} \text{Supp}_{\text{Bayes}}(r) \cdot \text{Conf}_{\text{Bayes}}(r) \quad (\text{F.14})$$

where r represents individual rules in configuration θ_k .

The prior probability $p(\theta_k | \mathcal{M}_k^{\mathbf{X_A} \rightarrow \mathbf{s}})$ reflects our beliefs about rule configurations within a model. For categorical variables in our green bond context, these priors can be informed by domain knowledge:

$$p(\theta_k | \mathcal{M}_k^{\mathbf{X_A} \rightarrow \mathbf{s}}) = \prod_{x_{i,k_i} \in \theta_k} P(x_{i,k_i}) \quad (\text{F.15})$$

where $P(x_{i,k_i})$ represents our prior belief about the importance of category k_i of attribute i . For example, if tax-exempt status (category $k = 1$ of the tax attribute) is believed to strongly influence spread behavior, we might assign a higher prior probability to $P(x_{\text{tax},1})$.

The model prior $P(\mathcal{M}_k^{\mathbf{X_A} \rightarrow \mathbf{s}})$ can be chosen to reflect preferences about model complexity. A common choice is:

$$P(\mathcal{M}_k^{\mathbf{X_A} \rightarrow \mathbf{s}}) \propto \exp(-\alpha|\theta_k|) \quad (\text{F.16})$$

where $|\theta_k|$ is the number of rules in configuration θ_k and $\alpha > 0$ is a complexity penalty parameter. This exponential penalty implements Occam's Razor by assigning higher prior probabilities to configurations with fewer rules, thereby favouring parsimonious explanations unless the data strongly supports more complex combinations of attribute categories.

Thus, our complete posterior probability can be written as:

$$\begin{aligned} P(\mathcal{M}_k^{\mathbf{X_A} \rightarrow \mathbf{s}} | D) &\propto \sum_{\theta_k} \left[\prod_{r \in \theta_k} \text{Supp}_{\text{Bayes}}(r) \cdot \text{Conf}_{\text{Bayes}}(r) \right] \\ &\times \left[\prod_{x_{i,k_i} \in \theta_k} P(x_{i,k_i}) \right] \exp(-\alpha|\theta_k|) \end{aligned} \quad (\text{F.17})$$

This framework balances three key components in model selection. First, the predictive power of rules is captured through their Bayesian Support and Confidence measures, reflecting how well each rule explains the observed relationships between one-hot encoded categories and spread outcomes. Second, domain expertise is incorporated through the prior

probabilities of individual categories $P(x_{i,k_i})$, allowing us to weight certain categories more heavily based on market knowledge. For instance, we might assign different prior probabilities to different coupon range categories ($P(x_{cpn,1})$ for 0-3%, $P(x_{cpn,2})$ for 3-5%, etc.) based on their expected importance in determining spread behavior. Third, the complexity penalty ensures that additional rules are only included when their explanatory power justifies the increased model complexity.

In practice, for our green bond analysis, this Bayesian model selection framework enables us to identify the most relevant combinations of one-hot encoded categories for predicting spread outcomes. The selected models represent those configurations of rules that best explain the observed data while maintaining a balance between model complexity and incorporation of market expertise through informative priors on bond characteristics. This approach is particularly well-suited to our categorical bond attributes, as it naturally handles the discrete nature of our one-hot encoded representation while incorporating domain knowledge about the relative importance of different attribute categories in determining spread behavior.

Appendix G. Labeling and attributes categories

The following table shows the details of the labeling process for each attribute.

Table G.1: Labeling process and details

Attribute	Labelling Approach	Labels
SPREAD MEDIAN EXTREME SPREAD	Sign of the annual median spread for each bond lower quantile of the annual spread distribution as the extreme negative, and the upper quantile as the extreme positive	S+, S-, S0 S(extreme-), S(extreme+)
MUNI_TAX_PROV	No revision was applied.	Tax: AMT/ST TAX-EXEMPT, FED & ST TAX-EXEMPT, FED BQ/ST TAX-E, FED TAX-EXEMPT, FED TAXABLE, FED TAXABLE/ST TAX-EXEMPT, FED TAXABLE/ST TAXABLE
SELF.REPTD.GREEN_INSTR.INDCTR ISSUER.BULK BB_COMPOSITE	"NA" was labelled as NA. No revision was applied. "NA" was labelled as NA.	Self Rep. Gr: NA, YES Issuer Name: Not included in the table BB.rating: A, A, A+, AA, AA-, AA+, AAA, BBB, BBB+, NA
MUNI_LONG_INDUSTRY_TYP	No revision was applied.	Issuer Sector: Airport, Bond Bank, Development, Education, General, General Obligation, Higher Education, Housing, Medical, Mello-Roos, Multifamily Hsg, Nursing Homes, Pollution, Power, School District, Transportation, Utilities, Water
CALLABLE MARKET_ISSUE	False: Non-Callable, True: Callable No revision was applied.	Call: Callable, Non-callable Market: CERTIFICATE PARTICIPATION, GENERAL OBLIGATION LTD, GENERAL OBLIGATION UNLTD, REVENUE BONDS, SPECIAL ASSESSMENT, SPECIAL TAX, TAX ALLOCATION
MUNI_PURPOSE	No revision was applied.	UOP: ADVANCE REFUNDING, CIVIC CONVENTION CENTER, CURRENT REFUNDING, ELEC. LT. & PWR. IMPTS., GREEN PURPOSE, HLTH-HOSP- NURSHOMES IMPS., MISC. PURPOSES, NURSING HOMES, PARKING FACILITY IMPS., PRT- AIRPRT & MARINA IMPS., PUBLIC FACILITIES, PUBLIC IMPS., RECREATIONAL FAC. IMPS., REFUNDING BONDS, REFUNDING NOTES, REPAYMENT OF BANK LOAN, RESOURCE RECOVERY IMPS., SCHOOL IMPS., SEWER IMPS., STATE MF HSG, STUDENT HOUSING, TRANSIT IMPS., UNIV. & COLLEGE IMPS., WATER UTILITY IMPS., FIN. Type: NEW MONEY, REFUNDING & NEW MONEY
FINANCING_TYPE	No revision was applied.	CPN: 0-3%, 3-5%, 5-8.5% SOID: less than 17, 17-57, 57-100, Higher than 100, NA
CPN_Group SPREAD_AT_ISSUANCE_TO_WORST DUR_Adj_MID	Labelled based on quartiles Labelled based on quartiles Labelled based on quartiles	DU_Adj_MID: less than 2.8, 2.8-4.8, 4.8-7, Higher than 7, NA
YIELD_ON_ISSUE_DATE	Labelled based on quartiles	Y_OID: less than 1.7, 1.7-2.4, 2.4-3.2, Higher than 3.2, NA
PRICING_TYPE AMT_ISSUED	Labelled based on the price compared to 100 Transformed into log scale and labelled based on the quartiles	Pricing TYP: At Discount, At Par, At Premium, NA Issued Amt: less than 14, 14-15, 15-16, higher than 16, NA
MUNI_ISSUE_SIZE	Transformed into log scale and labelled based on the quartiles	Muni Issued Size: 17-18.7, 18.7-19.5, higher than 19.5, less than 17
MTY_YEARS	Labelled based on quartiles	Maturity OID: less than 8, 12.3-17, 8-12.3, higher than 17
REMAINING_YEARS_TO_MATURITY	The year fraction between the calculation date and the maturity date of the bonds is computed and labeled according to the distribution quantiles of the calculated year fraction.	R_Ys to Maturity : Less than 4.7, 4.7-9.4, 9.4-14.4, Higher than 14.4
ACTIVE_YEARS	The year fraction between the calculation date and the issue date of the bonds is computed and labeled according to the distribution quantiles of the calculated year fraction.	Active years: Less than 1.1, 1.1-2.3, 2.3-4.1, Higher than 4.1

Appendix G.1. Labeling process, parameters setting and model order selection

To apply ARL we perform the following preparation steps. First, we categorize the attributes (defined in [Appendix A](#)) according to their characteristics and assign appropriate labels through a systematic labeling process for categorical and numerical attributes, as detailed in Table [G.1](#). The next step involves determining suitable thresholds that generate possible rules for positive and negative spreads. These thresholds are based on the first confidence quantiles of all rules in our itemsets, allowing us to discover rules with the highest confidence level within the most frequent ones in the dataset, which we refer to as strong rules.

The process of generating general rules and selecting parameter thresholds is detailed in next subsection. We set a *min_supp* of 0.1 for both positive and negative spreads and a *min_conf* thresholds of 0.56 for positive rules, and 0.45 and 0.49 for negative rules, respectively. After implementing the corresponding thresholds for positive and negative spreads, we obtained subsets of rules for positive and negative spreads, spanning orders 2 to 5. We use version 1.7-7 of the arules package in R, which includes the Apriori, Eclat, and FP-Growth algorithms for mining association rules and frequent itemsets. More specifically, we used the Apriori algorithm in this research ([Hahsler et al., 2023](#)). Within the context of the *arules* package in R, “order 2” signifies rules with one item in the antecedent (*lhs*) and one item in the consequent (*rhs*).

Appendix G.2. Threshold setting for the Apriori Algorithm

We initially set the parameters quite low, at 0.001 for both support and confidence, to generate all possible rules. The scatterplots below depict these rules at the specified parameter levels for positive and negative spreads.

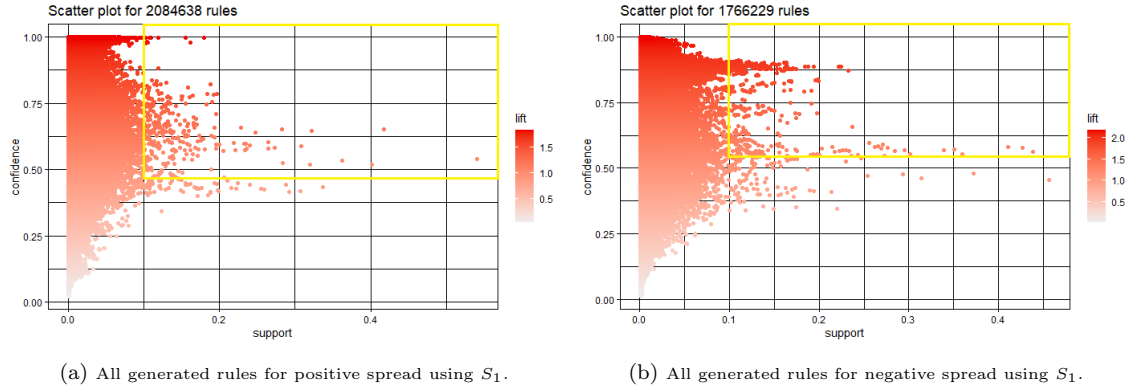


Figure G.1: All generated rules.

Incorporating a 10 percent threshold for support, we adopt a dynamic approach that utilizes the first quantile of the confidence distribution for positive and negative spreads. This consistent approach across spreads helps address the different characteristics of them. This adjustment ensures the identification of a suitable number of rules for both positive and negative scenarios, enhancing the robustness of our findings.

Table G.2 shows the descriptive statistics for confidence levels.

Table G.2: Summary statistics for all generated confidence levels

Spread	Descriptive Statistics					
	Min.	1st Qu.	Median	Mean	3rd Qu.	Max.
$S(+)$	0.0217	0.5613	0.7717	0.7383	0.9959	1.0000
$S(-)$	0.0114	0.4897	0.7219	0.6783	0.8819	1.0000

Appendix G.3. Bayesian model selection (BMS)

Lastly, to determine the order of the model through BMS (see Appendix F.3), we assume a uniform distribution for prior probabilities and model parameters. In association rule learning, “order” refers to the number of items (variables) involved in a rule. In the context of the arules package in R, “order 2” specifically indicates rules with one item in the antecedent (LHS) and one item in the consequent (RHS). In this paper, for simplicity, we start the rule order at 1, denoting only the number of itemsets in the LHS.

The table below reports the posterior probabilities of positive and negative rules by order.

Table G.3: Posterior probabilities for model order

Order	Posterior probability ($S(+)$)	Posterior probability ($S(-)$)
1	0.4697	0.4241
2	0.4814	0.4754
3	0.4678	0.5201
4	0.4592	0.5646

Using the conditional probability of the rules (confidence) within each order, we compute the posterior probabilities for each model order, see Table G.3. Accordingly, the posterior probability of models with positive spreads decreases as the model order increases, while the opposite trend is evident for negative spreads. Note that we perform the model for all generated rules in different orders. Given the minimal difference between model orders, we examine all orders, with particular attention to those showing higher posterior probabilities.

Appendix H. ANOVA method and results

To verify the statistical significance of the ARL results (order 2), we perform a one-way ANOVA test on the frequently identified attributes. To define subsamples for the ANOVA test, we categorize according to maturity (Maturity_OID), which is a common frequent

attribute previously identified.² We then investigate whether the contributions of the levels of other strong attributes to the spread variation are statistically significant.³

Appendix H.1. Samples

In this step, we take Maturity_OID to separate green bonds in different groups (indexed by i) in order to investigate the variance contribution of identified attributes (indexed by j) to the median of spreads within maturity categories. We have four maturity categories: *Less than 8*, *8_12.3*, *12.3_17*, and *Higher than 17*, and eight attributes: *MUNI_TAX_PROV*, *Pricing_TYP*, *CPN_range*, *S_OID*, *Y_OID*, *DAM*, *CALLABLE*, and *Issued_Amt*.

For each combination of maturity category and attribute, we conduct an ANOVA test to determine if there is a statistically significant difference contributed by attribute categories to each maturity group. Our sub-samples consist of bonds belonging to category k of attribute j within maturity group i , and we define their mean as μ_k^{ij} , where $k = 1, 2, \dots, c$ and c is the number of categories within attribute j .

Appendix H.2. Hypotheses

We define the null and alternative hypotheses for the ANOVA test as follows:

$$H_0 : \mu_1^{ij} = \mu_2^{ij} = \dots = \mu_c^{ij} \quad \text{for each pair of } i \text{ and } j$$

$$H_1 : \text{At least one pair of means is not equal for each pair of } i \text{ and } j$$

The following table summarizes the p-values obtained from the test, indicating the contribution of attributes to spread variation within each specific maturity group.

²We categorized green bonds based on their maturity since this characteristic affects the Investor's decision to manage convexity risk in fixed income investments. Also, maturity impacts the liquidity, with longer-term bonds experiencing higher demand due to reduced trading activity and investor preference for longer-term investments.

³Since we categorized green bonds according to Maturity_OID, we didn't include the other maturity-related attribute, R_Ys_to_Maturity, in the ANOVA test.

Table H.1: ANOVA p-values of bond attributes across maturity groups

Attributes	Maturity: Less than 8 ys	Maturity: 8.12.3 ys	Maturity: 12.3-17 ys	Maturity: Higher than 17 ys
MUNI_TAX.PROV	< 0.0e+00***	< 0.0e+00***	< 0.0e+00***	< 0.0e+00***
Pricing_TYP	< 0.0e+00***	< 0.0e+00***	< 0.0e+00***	< 0.0e+00***
CPN_range	< 0.0e+00***	< 0.0e+00***	< 2.6e-20***	< 2.2e-68***
S_OID	< 0.0e+00***	< 0.0e+00***	< 0.0e+00***	< 0.0e+00***
Y_OID	< 0.0e+00***	< 0.0e+00***	< 4.8e-213***	< 0.0e+00***
DAM	< 1.8e-70***	< 1.4e-153***	< 1.0e-69***	< 3.8e-201***
CALLABLE	< 6.2e-67***	< 1.3e-54***	< 2.2e-147***	< 0.0e+00***
Issued_Amt	< 1.9e-66***	< 5.9e-91***	< 1.1e-60***	< 7.5e-209***

Signif. codes: 0 ‘***’ 0.001 ‘**’ 0.01 ‘*’ 0.05 ‘.’ 0.1 ‘ ’ 1

Appendix H.3. Boxplot for spread variations

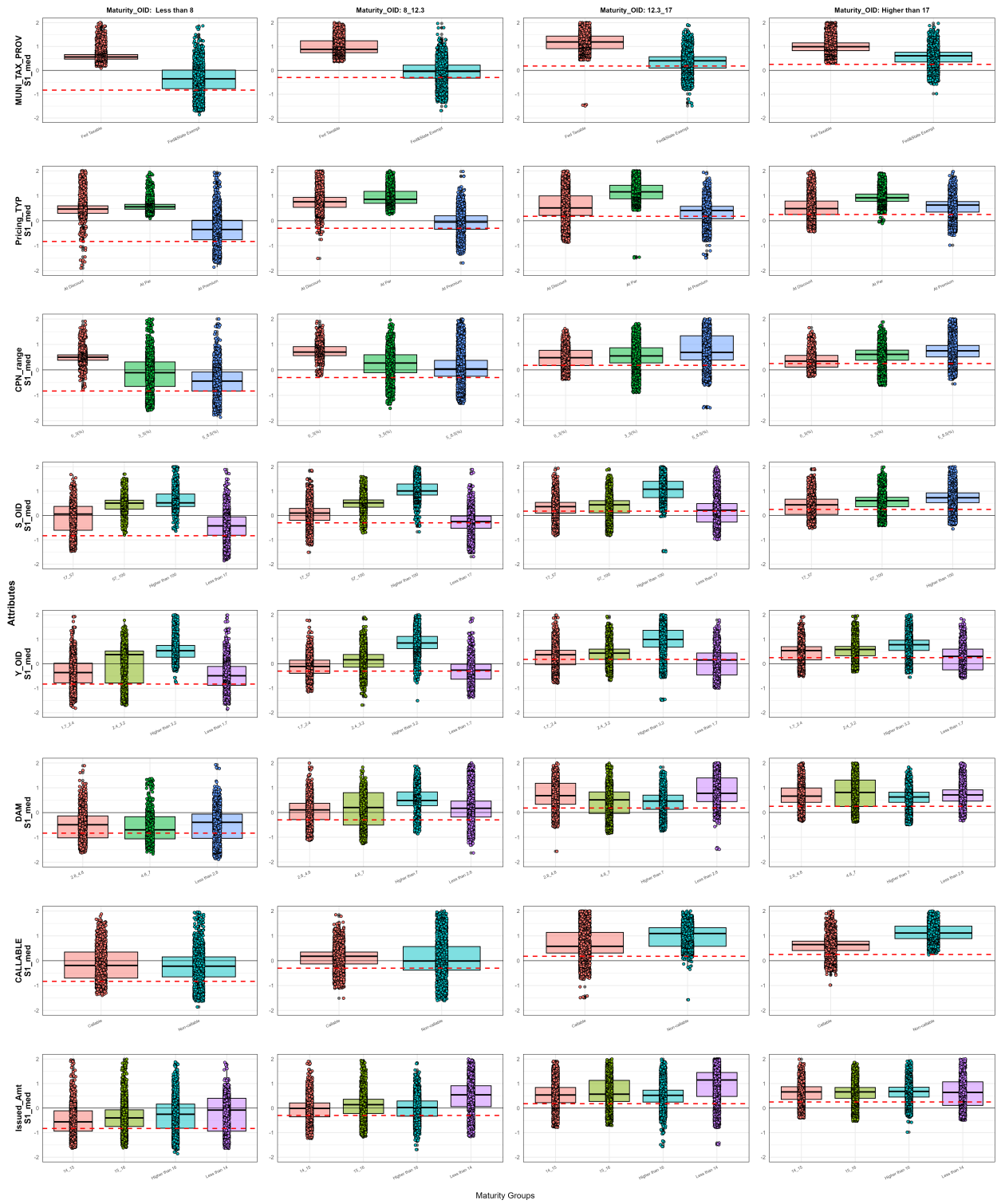


Figure H.1: Box plots for spread variation based on attributes

We find that the null hypothesis for all ANOVA tests for the top seven attributes can be rejected in favor of the alternative hypothesis (H1). More specifically, the contribution of tax status and at-par pricing type remains relatively stable across maturities. However, the contribution of the low coupon range to spread variation is more pronounced in short maturities and decreases as maturities increase. The S_OID and Y_OID play a greater role in spread variation in short maturities, whereas bonds with higher duration contribute more to spread variation in longer maturities, and vice versa. Furthermore, for longer-term bonds, the callability contributes to the spread variation. The issued amount only contributes to the variance in spreads at higher maturities, and the null hypothesis of the ANOVA test cannot be rejected for the first three maturity categories.

Appendix I. Parallel coordination for higher-order and extreme spreads

Appendix I.1. Parallel coordination for higher-order and extreme spreads

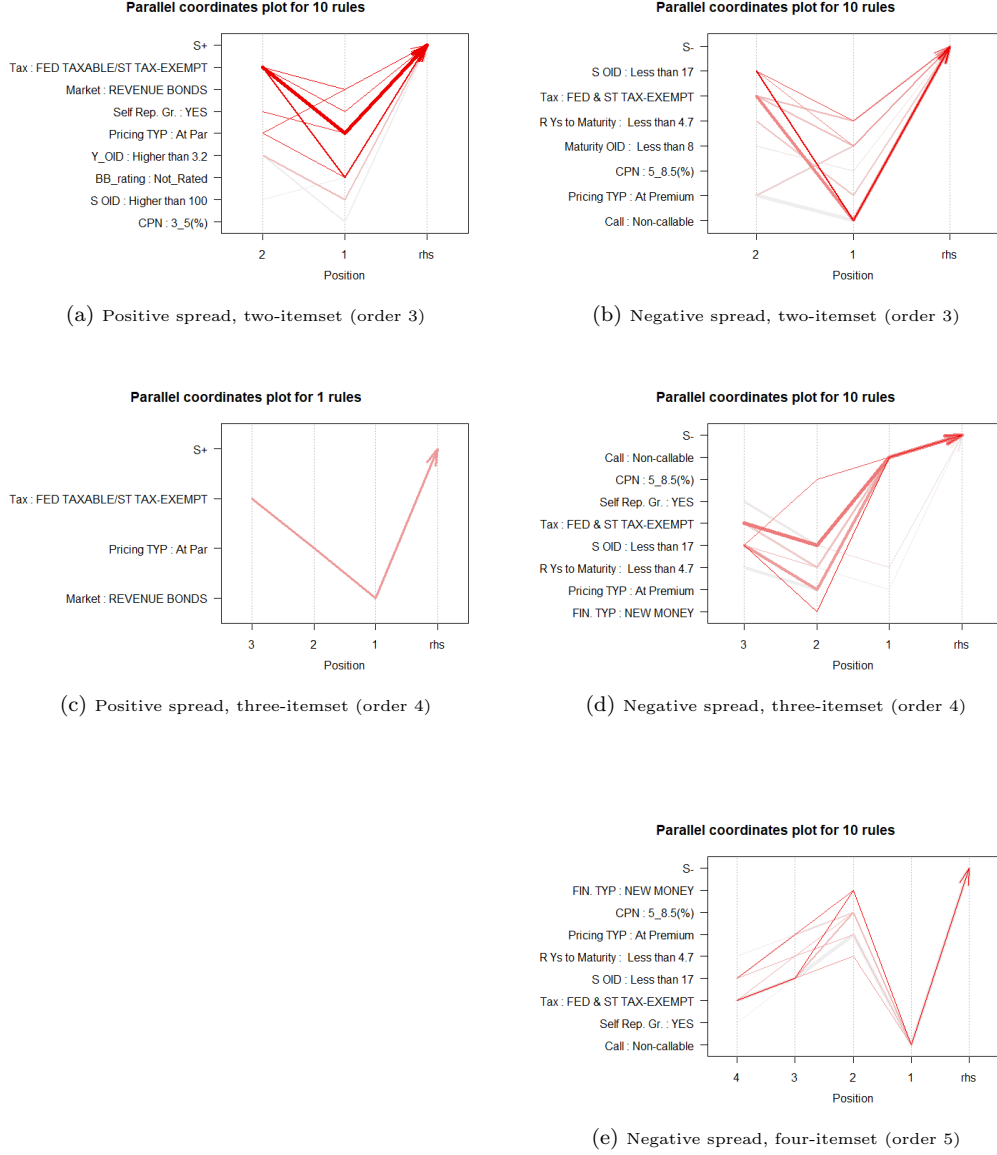


Figure I.1: Parallel coordination for model order for positive (left) and negative (right) green bond yield spreads.

This figure compares parallel-coordinated plots illustrating the relationships between different attributes across the model's ordered positions for positive (left column) and negative spreads (right column). The top row represents the top rules for the yield spreads using two-itemsets (order 3). The second row represents spread using three-itemsets (order 4). The bottom row shows the negative-spread rules using four-itemsets (order 5); there is no corresponding positive plot in that row. Color intensity indicates confidence, while line thickness represents rule support.

Appendix I.2. Parallel coordination for extreme spreads

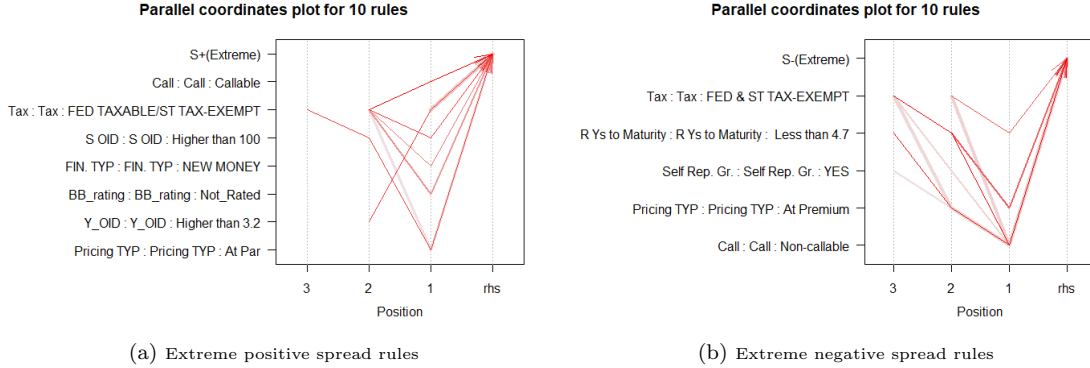


Figure I.2: Parallel coordination for extreme values of positive and negative green bond yield spreads.

This figure shows parallel coordinate plots for top ten extreme positive (negative) rules. Color intensity indicates confidence, while line thickness represents rule support.

Appendix J. Assessment within bonds with specific attributes

Appendix J.1. Assessment within bonds with specific attributes

In this appendix, we condition *LHS* of the rules on specific attributes or on a particular state (or category) of an attribute. This allows us to examine the attribute associations of green bond spreads within a particular type/group of green bonds. As the analysis above demonstrate, callability and tax status of green bonds are critical structuring attributes, thus we next assess attribute associations of positive and negative green bonds of a certain callability and tax status.

Appendix J.1.1. Callability-based attribute associations

Fig. J.1 displays the most frequent callability-based attribute associations for positive and negative spreads. We find that callable bonds that are tax-exempt or issued at a premium are more likely to have a positive spread. In addition, longer maturity remains a stable attribute associated with positive spread within callable bonds.

For non-callable bonds with a positive spread, the strongly associated attributes are the same across both spreads and include federal taxable bonds, bonds issued at par, and bonds with low coupon range. In terms of negative spreads of non-callable bonds, tax status, and pricing at premium matter for both spreads.

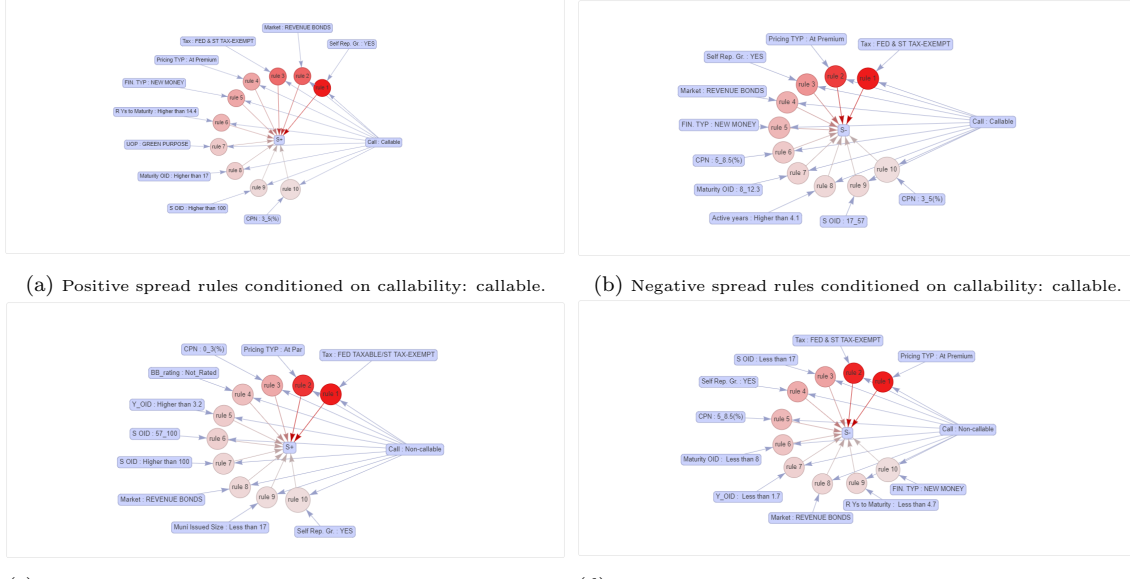


Figure J.1: Callability based rules for positive and negative green bond yield spreads.

This table presents the frequent rules of positive and negative spreads based on callable (top panels), non-callable bonds (second row panels). The left panels are for the positive spreads, the right panels are for the negative spreads.

Appendix J.1.2. Tax-based attribute associations

The more frequent attributes for tax-based (federally taxable or tax-exempt) associations are presented in Fig. J.2. Regarding attributes of federally taxable green bonds, we find that these green bonds, when issued at par, are strongly associated with positive spreads with other important attributes, including being self-reported as green, having no credit rating, and being issued as revenue bonds.

The attributes of tax-exempt green bonds with positive spreads include callability, issued at a premium, self-reported green, long maturity, and a high coupon range. Tax-exempt green bonds with negative spreads exhibit strong associations with bonds issued at premium or with low maturities. Spread at issuance gains more importance for yield spreads.

Generally, it is evident that callability and tax status are closely associated attributes of green bond yield spreads. More specifically, high-maturity and callable tax-exempt bonds, especially those issued at a premium, or federally taxable green bonds, especially when issued at par tend to have positive spreads. For the negative spreads, non-callable bonds, those issued at premium, or with low maturities tend to have negative spreads for both federally taxable and tax-exempt green bonds. A higher coupon rate emerges as a strong structuring

attribute of negative spreads, particularly in federally taxable bonds.

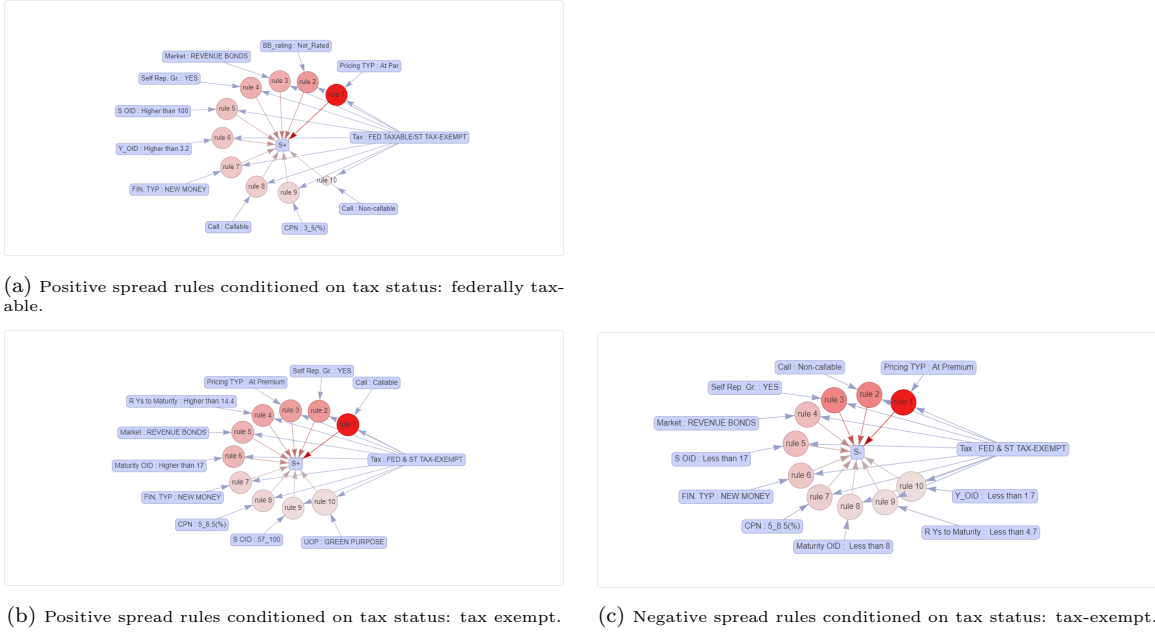


Figure J.2: Tax status-conditioned rules for positive and negative spread.

The left-column panels show rules conditioned on (i) federally taxable bonds (row 1) and (ii) tax-exempt bonds (row 2) for the positive spread. The right-column panel in row 2 shows the corresponding tax-exempt rule for the negative spread.

Appendix J.1.3. Attribute associations based on bond's issuer sector

We identify the attribute associations of positive and negative spreads from a specific green bond issuer sector. We select issuer sectors with more than 100 green bonds, including General, Water, General Obligation, School District, Power, and Pollution.

Figures J.3 and J.4 present the most frequent attributes of positive and negative green bond spreads of certain issuer sectors. Accordingly, attributes related to the issued size and amount are frequent in (positive and negative) spreads together with maturity-related attributes (including Active years, maturity_OID, and remaining years to maturity). Credit rating is frequent among green bonds with positive spreads in the Water and Pollution sectors and for negative spreads in the General and Water sectors. Tax is common in the Energy, Pollution and Utilities sectors, while callability is a dominant attribute mostly for negative spreads in School District, Pollution, General Obligation, and Utilities. Specifically, in the Power, Utilities, and Pollution sector, self-reported bonds and financing type (refund or new money) are the most frequent attribute with negative spreads.

Thus, green bond yield spreads based on issuer sectors are associated with the classical tax and callability attributes, yet credit rating, issued amount, and maturity related attributes are also critical, especially for negative spreads.

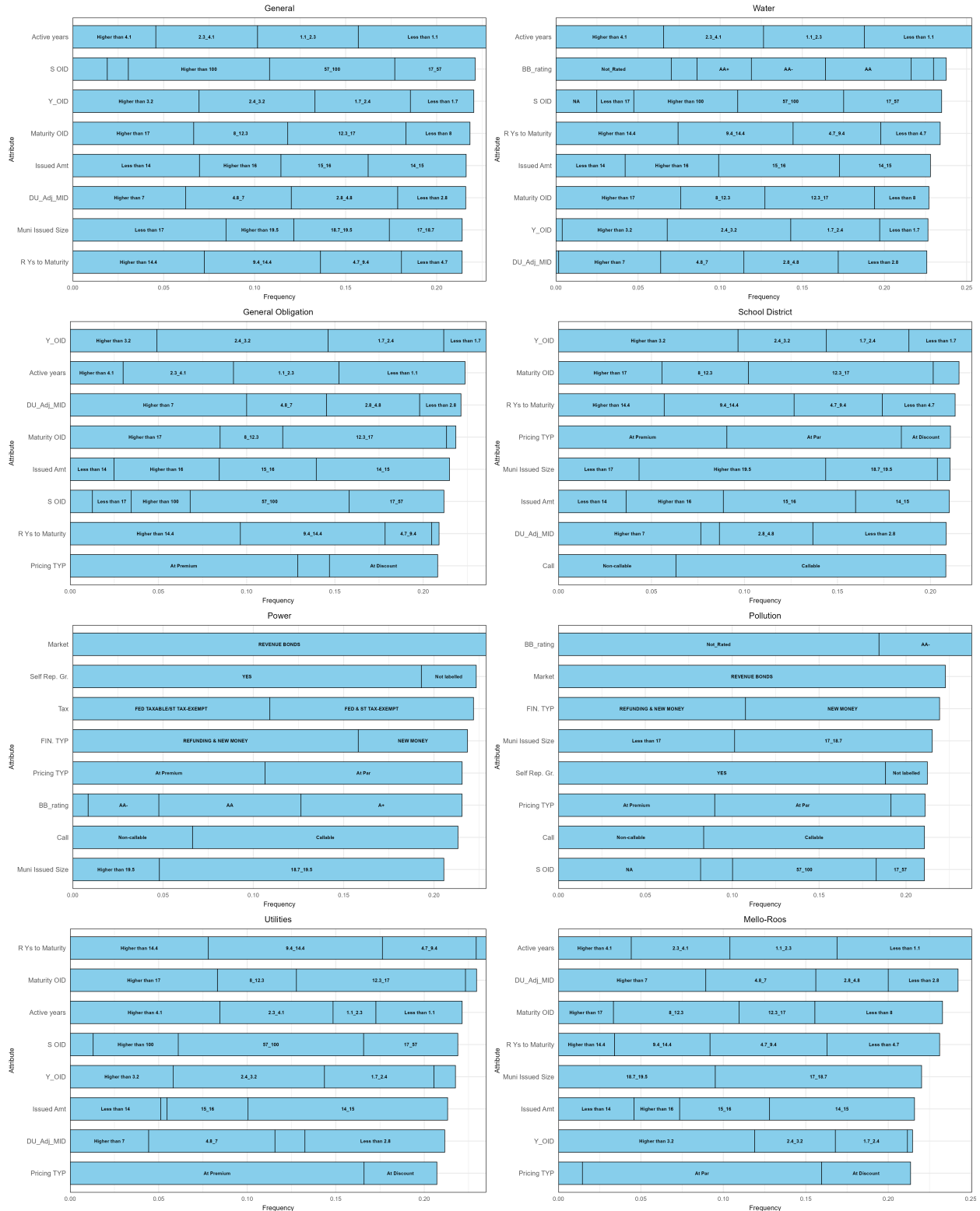


Figure J.3: Frequency of attributes within certain issuer sector.
This plot shows the frequency of rules for positive spread within a certain issuer sector.

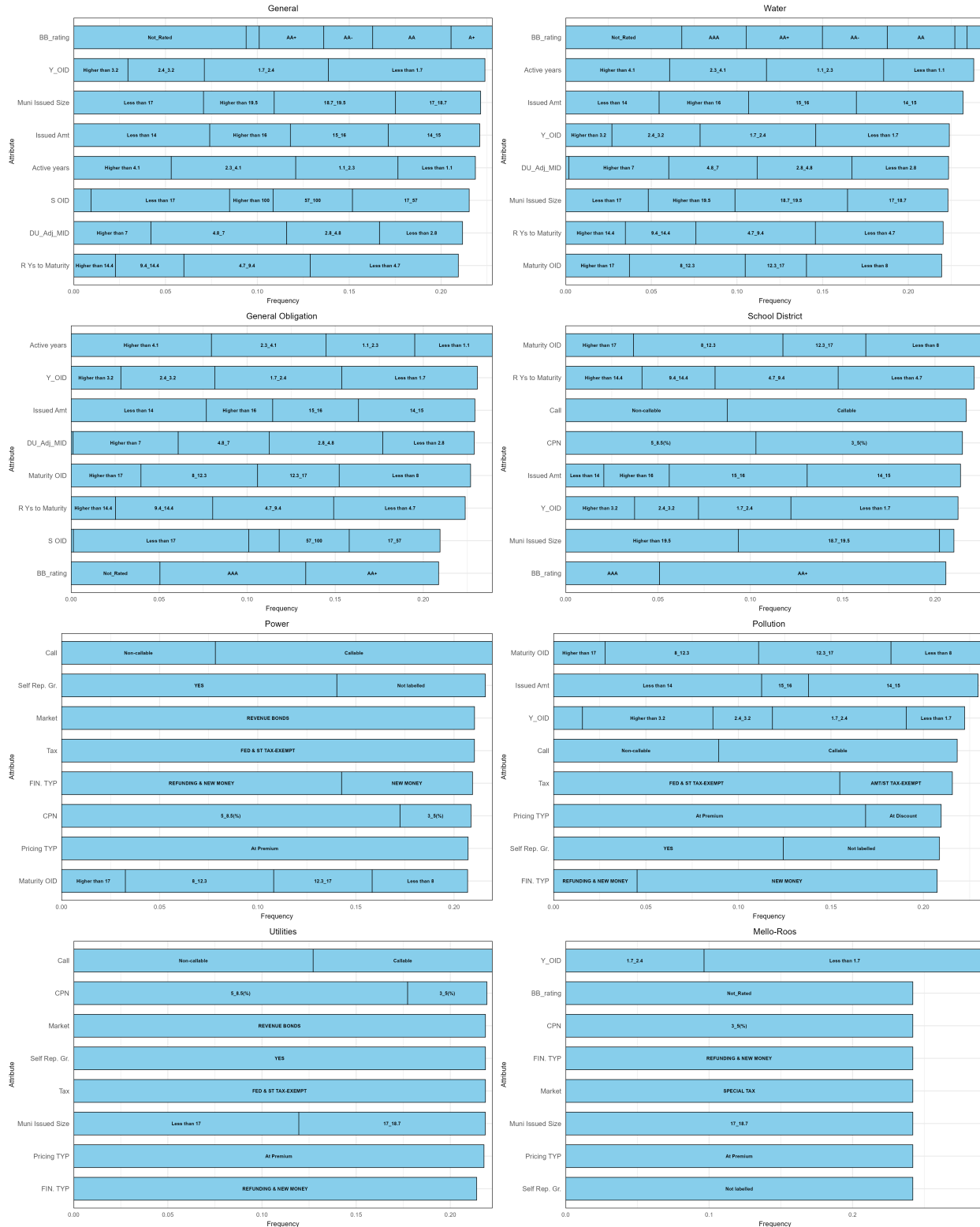


Figure J.4: Frequency of attributes within certain issuer sector.
This plot shows the frequency of rules for negative spread within a certain issuer sector.

Appendix J.2. UOP definition

BBG does not offer specific definitions for municipal UOPs. To ensure clarity and accuracy, we relied on multiple external references to compile comprehensive and precise definitions for each UOP category included in our dataset. We collected the definitions for UOPs in our dataset from a variety of reputable online sources.

Table J.1: Terms, Definitions, and Sources

Term	Definition	Source
CURRENT REFUNDING	Refunding of a bond within 90 days of the call date, typically done to take advantage of lower rates.	http://www.msrb.org/Glossary/Definition/REFUNDING.aspx
WATER UTILITY IMPROVEMENTS	Investments in infrastructure related to water supply, treatment, and distribution systems.	https://www.epa.gov/dwsrf/water-infrastructure-improvements-water-systems
ADVANCE REFUNDING	Issuing new bonds to replace old ones before the call date, using the proceeds to retire the original bonds.	http://www.msrb.org/Glossary/Definition/ADVANCE-REFUNDING.aspx
TRANSIT IMPROVEMENTS	Enhancements to public transportation infrastructure—buses, subways, and rail systems.	https://www.transit.dot.gov/grants
PUBLIC IMPROVEMENTS	Improvements to public facilities—roads, parks, and community centers.	https://www.gfoa.org/capital-improvement-plan
SCHOOL IMPROVEMENTS	Upgrades and repairs to educational facilities, building or renovating schools.	https://www.ed.gov/school-improvement
PUBLIC FACILITIES	Construction and maintenance of government buildings and community centers.	https://www.nlc.org/program-initiative/community-economic-development
REFUNDING NOTES	Short-term notes issued to temporarily finance the refunding of longer-term debt.	http://www.msrb.org/Glossary/Definition/NOTES.aspx
SEWER IMPROVEMENTS	Upgrades and expansion of sewage and wastewater treatment infrastructure.	https://www.epa.gov/npdes/municipal-wastewater
ELECTRIC LIGHT & POWER IMPS.	Investments in electric-utility infrastructure: generation, transmission, distribution.	https://www.eia.gov
RECREATIONAL FACILITY IMPS.	Investments in parks, sports complexes, and other recreational facilities.	https://www.nrpa.org/

Appendix J.2.1. UOP-based attribute associations

Note that different sectors are issuing green bonds with various UOPs.⁴ ⁵ For a more complete assessment, we also examine the attribute associations of green bond yield spreads of different UOPs. The definitions of the UOP used in our analysis are summarized in Table J.1. Figures J.5 shows the attributes of positive and negative spreads for different UOPs.

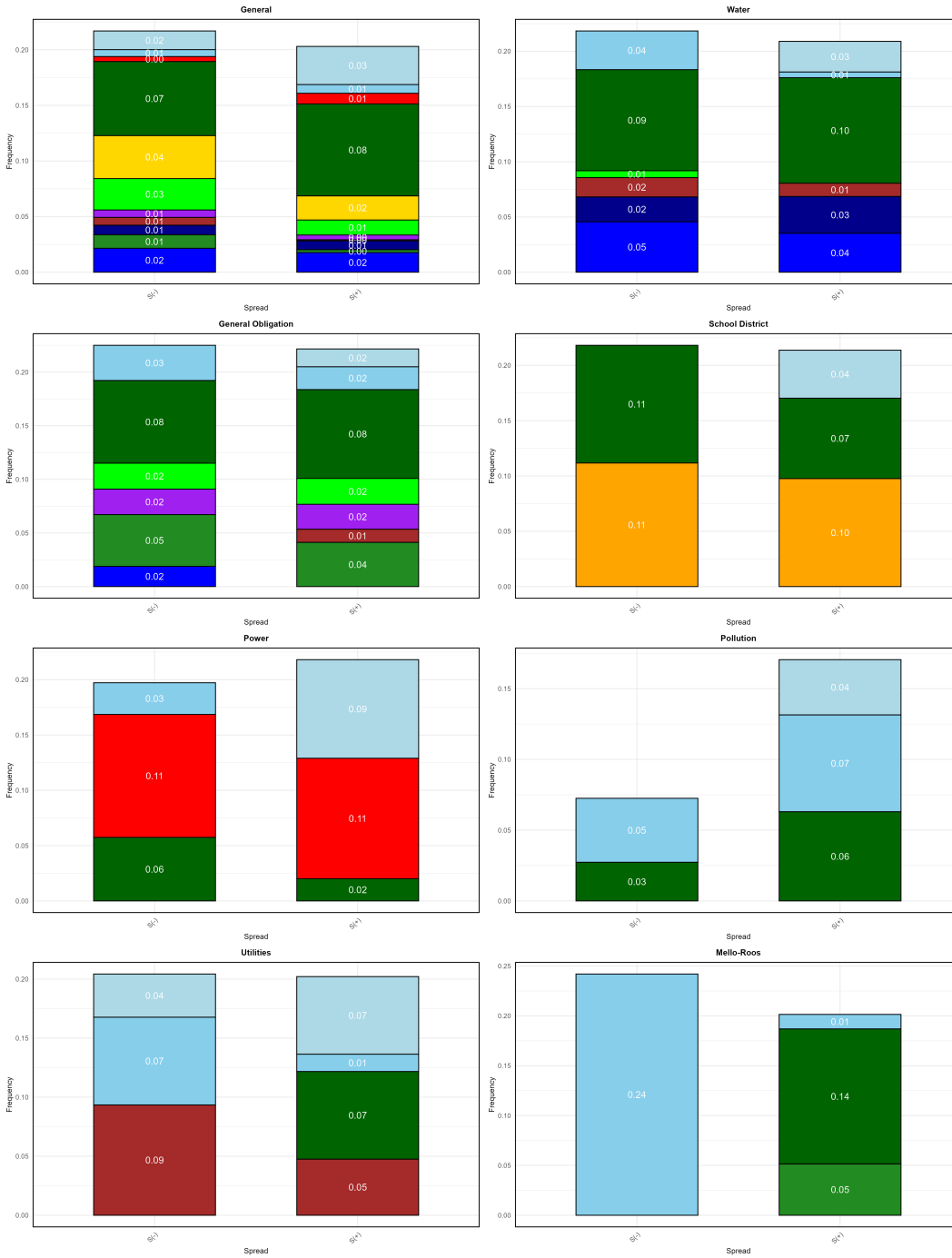
We find that Green Purpose is the most frequent UOP across sectors, appearing more

⁴This feature is often included in the issuance prospectus and may provide specific details about the project, environmental impact reports, and second- or third-party assurances. However, it can sometimes be vague. These details influence green index ratings and listings. Currently, specific mandates regarding the use of raised capital have not been legally enshrined as protections in the form of hard green covenants.

⁵Different sectors have varying environmental impacts, affecting the environmental benefits associated with green bonds. However, the UOP indicates how funds raised through green bonds will be used, providing clarity on the specific environmental projects or activities financed by the bonds. The UOP information improves transparency and accountability, helping investors assess the environmental impact of green bond projects. From an investment point of view, the UOP and issuer sector may also impact the risk of default and repayment. Investigation of these attributes can provide investors with valuable insights for their investment decisions (Benlemlih et al., 2023; Russo et al., 2021).

often in positive spreads, except in the Power and School District sectors. In the General, Water, and General Obligation sectors, Green Purpose is prevalent in both positive and negative spreads, though it appears more frequently in positive spreads. In contrast, the General Obligation sector shows a notable trend, with Current Refunding dominating negative spreads and Green Purpose being less frequent in positive spreads.

In the School District sector, School Improvements is the most common UOP, significantly more frequent in positive spreads. The Power sector shows Electricity Lights and Power Improvements (ELEC. LT. & PWR. IMPTS) as the dominant UOP, with a higher share in positive spreads. In the Pollution and Utilities sectors, refunding-related UOPs (Current Refunding and Refunding Notes) are more frequent in negative spreads, while Green Purpose has a smaller presence in positive spreads across both sectors.



Use of Proceeds (UOP)

ADVANCE REFUNDING	GREEN PURPOSE	RECREATIONAL FAC IMP'S	SEWER IMP'S.
CURRENT REFUNDING	PUBLIC FACILITIES	REFUNDING NOTES	TRANSIT IMP'S.
ELEC. LT. & PWR. IMP'TS.	PUBLIC IMP'S.	SCHOOL IMP'S.	WATER UTILITY IMP'S.

Figure J.5: Frequency of attributes within certain UOPs in sectors.

This table shows the frequency of rules for positive and negative spread within certain UOPs in sectors. The left panels are for the negative spreads, and the right panels are for the positive spreads.

Appendix K. Regression model plots and tests

Appendix K.1. Issue date interval analysis

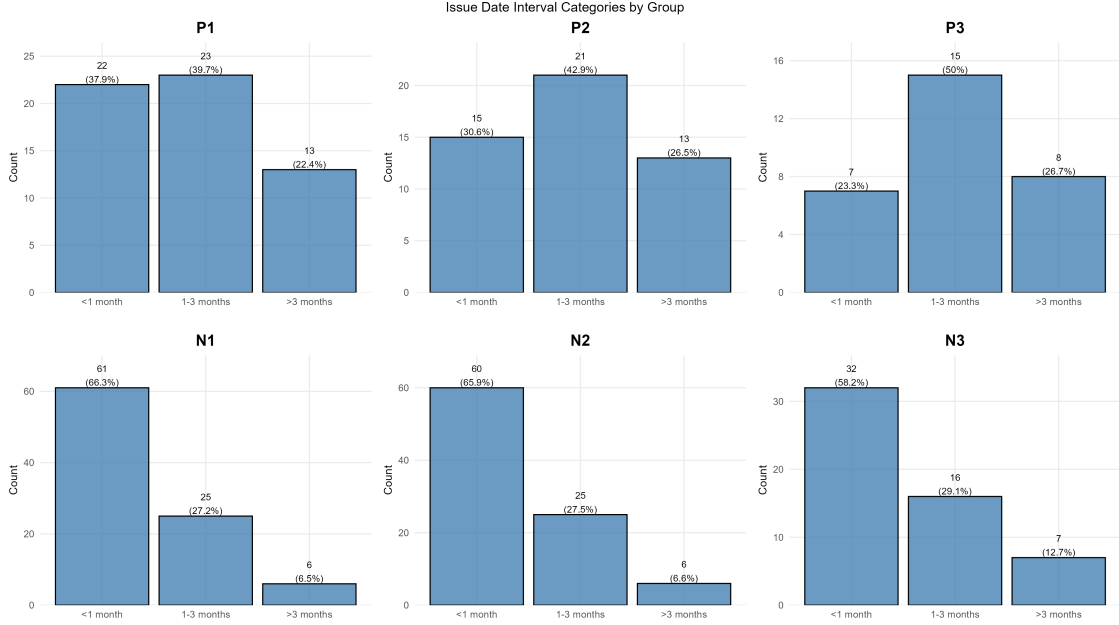


Figure K.1: General distribution of issue date intervals across bond groups. The plot shows the frequency of different time intervals between consecutive bond issues for each association rule group. Categories represent intervals of less than 1 month, 1-3 months, and greater than 3 months. P2, P3, P4 represent positive spread rules of increasing complexity, while N2, N3, N4 represent negative spread rules of increasing complexity.

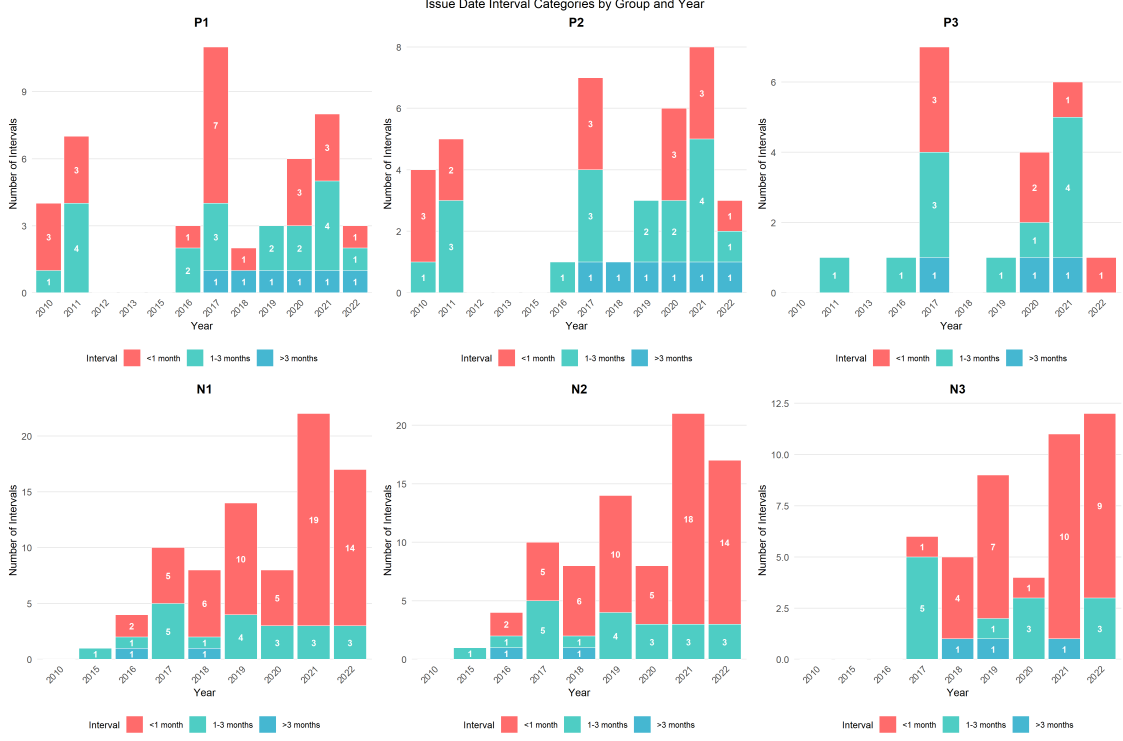


Figure K.2: Yearly distribution of issue date intervals across bond groups. The stacked bar charts show the frequency of different time intervals between consecutive bond issues within each year for each association rule group. Each bar segment represents intervals of less than 1 month (red), 1-3 months (teal), and greater than 3 months (blue), with counts displayed on each segment. P1, P2, P3 represent positive spread rules of increasing complexity, while N1, N2, N3 represent negative spread rules of increasing complexity. The temporal breakdown reveals how bond issuance patterns evolved over time within each rule-based group.

Appendix K.2. Correlation heatmaps for bonds groups.

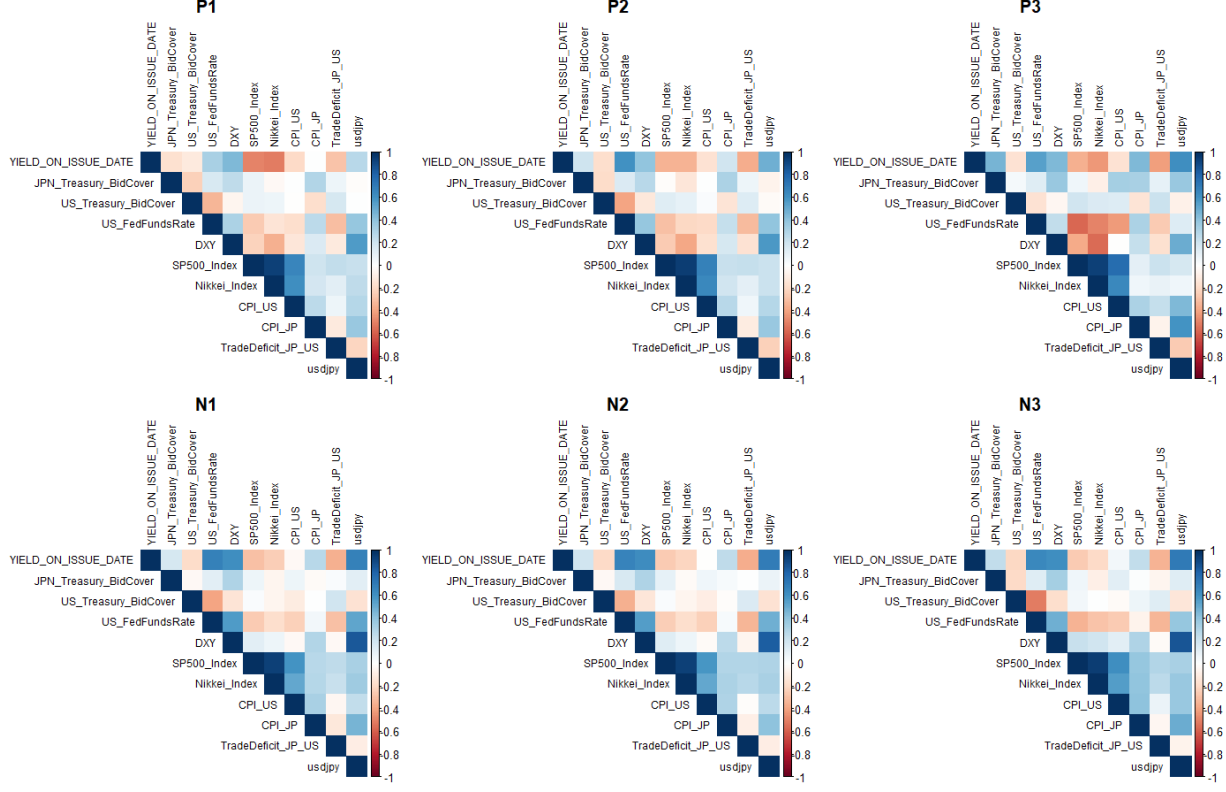


Figure K.3: Correlation heatmaps for six bond association rule groups. The upper triangular matrices show pairwise correlations between all regression variables for each group. The top row displays positive spread groups (P1, P2, P3) representing rules of increasing complexity that predict positive yield spreads. The bottom row shows negative spread groups (N1, N2, N3) representing rules of increasing complexity that predict negative yield spreads. Color intensity indicates correlation strength, with darker colors representing stronger correlations.

Appendix K.3. Tests and diagnostic plots

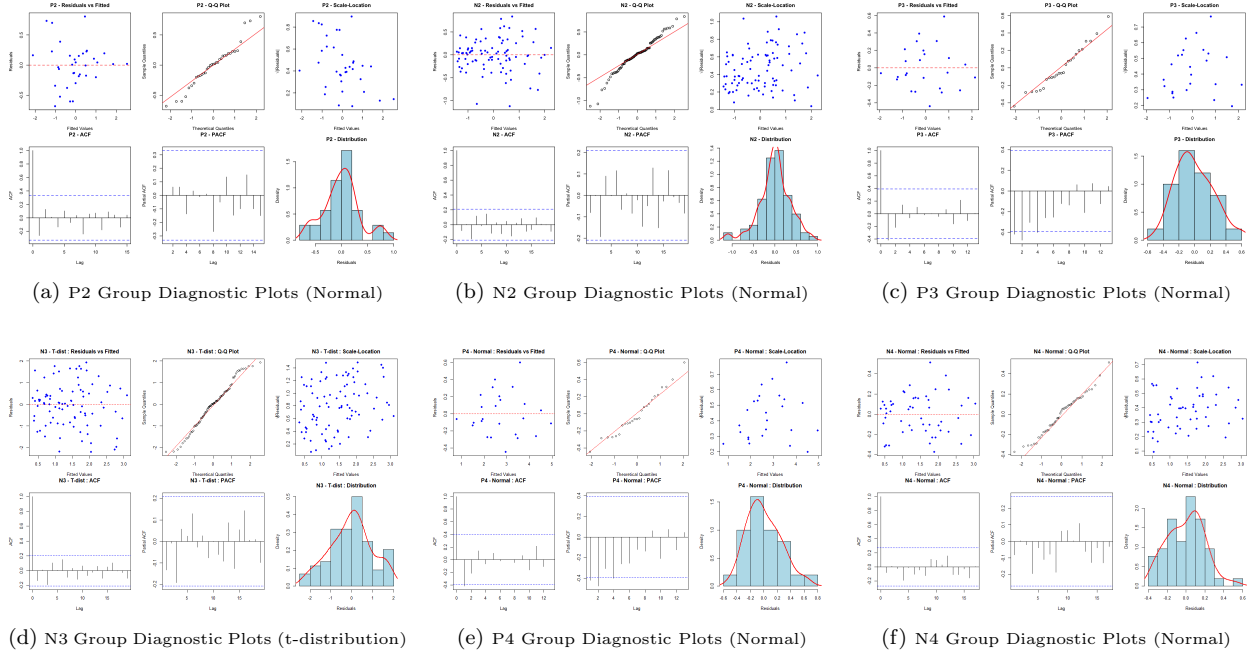


Figure K.4: Diagnostic plots for the lagged dynamic linear models fitted to Japanese municipal bond yields across different maturity and issuer groups. Each subplot contains six diagnostic plots: residuals vs fitted values, Q-Q plot against theoretical distribution, scale-location plot, autocorrelation function of residuals, partial autocorrelation function, and residuals distribution comparison. Groups P2, N2, P3, P4, and N4 use normal error distributions, while group N3 employs Student's t-distribution based on excess kurtosis analysis. The plots validate model assumptions including homoscedasticity, distributional adequacy, and absence of serial correlation in residuals.

Table K.1: Comprehensive residual diagnostic tests. LB = Ljung-Box test for serial correlation (H_0 : no serial correlation). SW = Shapiro-Wilk test for normality (H_0 : residuals are normal). BP = Breusch-Pagan test for homoscedasticity (H_0 : constant variance). p-value > 0.05 indicates acceptance of null hypothesis. Test lag for LB chosen as $\min(10, n/5)$ where n is sample size. SW test not performed for $n > 5000$.

Group	N	Serial Correlation			Normality			Homoscedasticity		
		LB Stat	p-value	White Noise	SW Stat	p-value	Normal	BP Stat	p-value	Homosced.
P1	38	5.529	0.596	Yes	0.983	0.808	Yes	15.601	0.552	Yes
N1	87	13.870	0.179	Yes	0.974	0.082	Yes	25.056	0.093	Yes
P2	35	4.778	0.687	Yes	0.960	0.228	Yes	14.255	0.649	Yes
N2	88	10.487	0.399	Yes	0.973	0.060	Yes	25.103	0.092	Yes
P3	25	7.408	0.192	Yes	0.971	0.659	Yes	12.608	0.762	Yes
N3	52	5.694	0.840	Yes	0.981	0.547	Yes	20.191	0.265	Yes

Appendix K.4. Results and diagnostic plots for N3_2 and N3_3

Table K.2: Lagged regression results for municipal bond yields. P1, P2, P3 represent positive spread groups of orders 1, 2, 3 respectively. N1, N2, N3, N3_2, N3_3 represent negative spread groups of orders 1, 2, 3, and groups of order 3 using second and third ranked rules, respectively. Significance levels: *** p<0.001, ** p<0.01, * p<0.05, . p<0.10. Standard errors are shown in parentheses.

	P1	P2	P3	N1	N2	N3	N3_2	N3_3
JPN_Treasury_BidCover	0.2247** (0.0781)	0.3279* (0.1225)	0.3970. (0.1745)	0.0645 (0.0625)	0.0785 (0.0612)	0.2557** (0.0737)	0.1589* (0.0741)	0.0848 (0.0629)
US_Treasury_BidCover	0.0313 (0.0696)	-0.0128 (0.1142)	0.0827 (0.1339)	0.0041 (0.0523)	0.0019 (0.0511)	0.0145 (0.0638)	0.0441 (0.0665)	0.0023 (0.0527)
US_FedFundsRate	0.2838. (0.1446)	0.4171 (0.2530)	0.3533 (0.3703)	-0.2204 (0.2916)	-0.2852 (0.2758)	-0.2884 (0.2122)	-0.1297 (0.2778)	-0.2218 (0.2933)
DXY	-0.4128* (0.1789)	-0.7056* (0.2850)	-0.6392. (0.3184)	-0.0472 (0.1817)	-0.0378 (0.1774)	0.6186** (0.1846)	-0.0923 (0.2133)	-0.0350 (0.1819)
SP500_Index	1.8779** (0.5145)	3.0237** (0.8737)	1.5776 (1.1499)	-0.3972 (0.3607)	-0.4544 (0.3500)	0.2717 (0.3118)	-0.7957* (0.3898)	-0.5372 (0.3638)
Nikkei_Index	-1.4312*** (0.3182)	-2.3051*** (0.5455)	-1.2035 (0.9710)	-0.0775 (0.2679)	-0.0142 (0.2613)	0.2514 (0.1998)	0.0745 (0.2789)	0.0371 (0.2687)
usdjay	0.9387*** (0.2074)	1.6295*** (0.3490)	1.0178** (0.2739)	0.6417* (0.2620)	0.6982** (0.2613)	-0.3215 (0.3212)	0.5445 (0.3369)	0.6424* (0.2659)
CPI_US	-0.1624. (0.0808)	-0.3196* (0.1414)	-0.5755. (0.2826)	0.0519 (0.0734)	0.0534 (0.0717)	0.0230 (0.0790)	0.0963 (0.0887)	0.0576 (0.0740)
CPI_JP	-0.0576 (0.0824)	-0.1201 (0.1342)	-0.0378 (0.1775)	0.0459 (0.0538)	0.0400 (0.0534)	0.1144. (0.0596)	0.0442 (0.0647)	0.0436 (0.0544)
TradeDeficit_JP_US	-0.1295. (0.0669)	-0.2244. (0.1148)	-0.2818 (0.2800)	-0.0164 (0.0530)	-0.0162 (0.0524)	-0.0105 (0.0530)	0.0003 (0.0622)	-0.0186 (0.0541)
YIELD_ON_ISSUE_DATE _{t-1}	-0.2419 (0.1602)	-0.3345. (0.1653)	-0.3603 (0.2849)	0.5213*** (0.1134)	0.5092*** (0.1103)	0.4920** (0.1416)	0.4337** (0.1403)	0.4845*** (0.1126)
YIELD_ON_ISSUE_DATE _{t-2}	-0.2975 (0.1952)	-0.4148. (0.2014)	-0.1679 (0.2305)	0.0066 (0.1239)	0.0085 (0.1188)	0.0611 (0.1351)	-0.0932 (0.1395)	0.0155 (0.1242)
US_FedFundsRate _{t-1}	0.0823 (0.1832)	0.2582 (0.3252)	0.1589 (0.5145)	0.2672 (0.2787)	0.3298 (0.2576)	0.2644 (0.2268)	0.1427 (0.2776)	0.2731 (0.2795)
DXY _{t-1}	-0.2042 (0.1833)	-0.3377 (0.2988)	-0.1440 (0.2971)	-0.1732 (0.1706)	-0.1944 (0.1659)	-1.0384*** (0.1698)	-0.2183 (0.2015)	-0.1924 (0.1712)
SP500_Index _{t-1}	-0.9901. (0.5088)	-1.4242 (0.8429)	-0.0518 (1.1521)	0.2028 (0.3422)	0.2193 (0.3314)	-0.6436* (0.2899)	0.1240 (0.3787)	0.2924 (0.3443)
Nikkei_Index _{t-1}	0.0003 (0.3422)	-0.2114 (0.5585)	-0.7151 (0.8230)	-0.0604 (0.2586)	-0.0975 (0.2535)	-0.1852 (0.1919)	0.0719 (0.2699)	-0.1418 (0.2589)
usdjay _{t-1}	-0.2499 (0.1876)	-0.2802 (0.3507)	0.0383 (0.3825)	-0.0430 (0.2341)	-0.0652 (0.2368)	1.1337*** (0.2972)	0.3331 (0.3107)	-0.0189 (0.2373)
Adjusted R ²	0.7369	0.7628	0.8066	0.8172	0.8413	0.9038	0.8109	0.8160

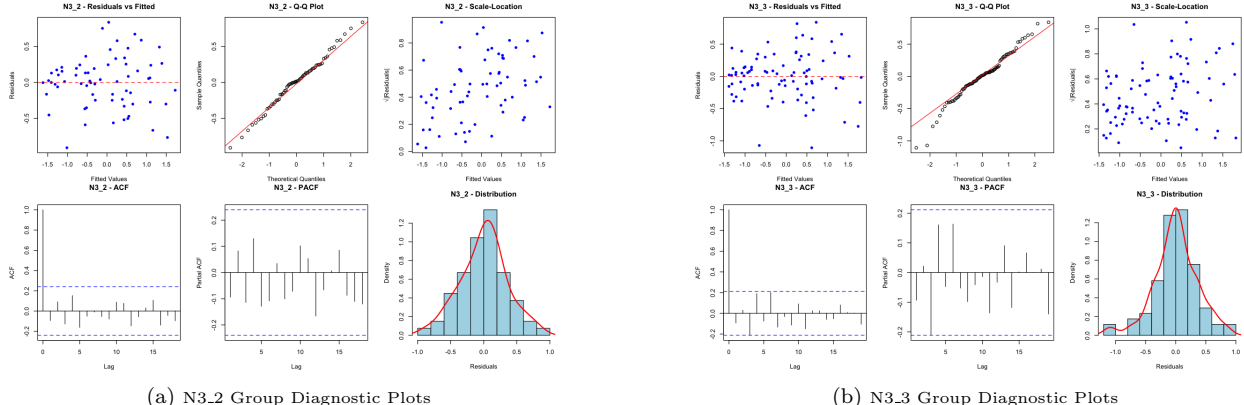


Figure K.5: Diagnostic plots for the lagged dynamic linear models fitted to Japanese municipal bond yields for the last two groups (N3_2 and N3_3). Each subplot contains six diagnostic plots: residuals vs fitted values, Q-Q plot against the theoretical distribution, scale-location plot, autocorrelation function of residuals, partial autocorrelation function, and residuals distribution comparison. Both groups employ Student's t-distribution based on excess kurtosis analysis. The plots validate model assumptions including homoscedasticity, distributional adequacy, and absence of serial correlation in residuals.

Table K.3: Comprehensive residual diagnostic tests. LB = Ljung-Box test for serial correlation (H_0 : no serial correlation). SW = Shapiro-Wilk test for normality (H_0 : residuals are normal). BP = Breusch-Pagan test for homoscedasticity (H_0 : constant variance). p-value > 0.05 indicates acceptance of null hypothesis. Test lag for LB chosen as $\min(10, n/5)$ where n is sample size. SW test not performed for $n > 5000$.

Group	N	Serial Correlation			Normality			Homoscedasticity		
		LB Stat	p-value	White Noise	SW Stat	p-value	Normal	BP Stat	p-value	Homosced.
N3_2	67	7.601	0.668	Yes	0.991	0.912	Yes	19.743	0.288	Yes
N3_3	86	16.615	0.083	Yes	0.976	0.109	Yes	23.870	0.123	Yes

References

- Agrawal, R., Imieliński, T., Swami, A., 1993. Mining association rules between sets of items in large databases, in: Proceedings of the 1993 ACM SIGMOD international conference on Management of data, pp. 207–216. doi:[10.1145/170035.170072](https://doi.org/10.1145/170035.170072).
- Benlemlih, M., Jaballah, J., Kermiche, L., 2023. Does financing strategy accelerate corporate energy transition? Evidence from green bonds. *Business Strategy and the Environment* 32, 878–889. doi:[10.1002/bse.3180](https://doi.org/10.1002/bse.3180).
- Diebold, F.X., Li, C., 2006. Forecasting the term structure of government bond yields. *Journal of Econometrics* 130, 337–364. doi:[10.1016/j.jeconom.2005.03.005](https://doi.org/10.1016/j.jeconom.2005.03.005).
- Hahsler, M., Buchta, C., Gruen, B., Hornik, K., 2023. arules: Mining Association Rules and Frequent Itemsets. R package version 1.7-7 <https://CRAN.R-project.org/package=arules>.
- Hastie, T., Tibshirani, R., Friedman, J.H., Friedman, J.H., 2009. The elements of statistical learning: data mining, inference, and prediction. volume 2. Springer.
- Russo, A., Mariani, M., Caragnano, A., 2021. Exploring the determinants of green bond issuance: Going beyond the long-lasting debate on performance consequences. *Business Strategy and the Environment* 30, 38–59. doi:[10.1002/bse.2608](https://doi.org/10.1002/bse.2608).
- Tian, D., Gledson, A., Antoniades, A., Aristodimou, A., Ntalaperas, D., Sahay, R., Pan, J., Stivaros, S., Nenadic, G., Zeng, X.j., et al., 2013. A bayesian association rule mining algorithm, in: 2013 IEEE international conference on systems, man, and cybernetics, IEEE. pp. 3258–3264. doi:[10.1109/SMC.2013.555](https://doi.org/10.1109/SMC.2013.555).
- Yallup, P.J., 2012. Models of the yield curve and the curvature of the implied forward rate function. *Journal of Banking & Finance* 36, 121–135. doi:[10.1016/j.jbankfin.2011.06.010](https://doi.org/10.1016/j.jbankfin.2011.06.010).